Bull Volcanol (1997) 59:198–218

ORIGINAL PAPER

P. W. Lipman

Subsidence of ash-flow calderas: relation to caldera size and magma-chamber geometry

Received: 13 February 1997 / Accepted: 9 August 1997

Abstract Diverse subsidence geometries and collapse processes for ash-flow calderas are inferred to reflect varying sizes, roof geometries, and depths of the source magma chambers, in combination with prior volcanic and regional tectonic influences. Based largely on a review of features at eroded pre-Quaternary calderas, a continuum of geometries and subsidence styles is inferred to exist, in both island-arc and continental settings, between small funnel calderas and larger plate (piston) subsidences bounded by arcuate faults. Within most ring-fault calderas, the subsided block is variably disrupted, due to differential movement during ash-flow eruptions and postcollapse magmatism, but highly chaotic piecemeal subsidence appears to be uncommon for large-diameter calderas. Small-scale downsag structures and accompanying extensional fractures develop along margins of most calderas during early stages of subsidence, but downsag is dominant only at calderas that have not subsided deeply. Calderas that are loci for multicyclic ash-flow eruption and subsidence cycles have the most complex internal structures. Large calderas have flared inner topographic walls due to landsliding of unstable slopes, and the resulting slide debris can constitute large proportions of caldera fill. Because the slide debris is concentrated near caldera walls, models from geophysical data can suggest a funnel geometry, even for large plate-subsidence calderas bounded by ring faults. Simple geometric models indicate that many large calderas have subsided 3–5 km, greater than the depth of most naturally exposed sections of intracaldera deposits. Many ring-fault plate-subsidence calderas and intrusive ring complexes have been recognized in the western U.S., Japan, and elsewhere, but no well-documented examples of exposed eroded calderas have large-scale funnel geometry or chaotically disrupted caldera floors. Reported ignimbrite "shields" in the central Andes, where large-volume ash-flows are inferred to have erupted without caldera collapse, seem alternatively interpretable as more conventional calderas that were filled to overflow by younger lavas and tuffs. Some exposed subcaldera intrusions provide insights concerning subsidence processes, but such intrusions may continue to evolve in volume, roof geometry, depth, and composition after formation of associated calderas.

Key words Volcanoes · Caldera geometry · Caldera subsidence · Ash-flow tuff

Editorial responsibility: M. Rosi

Peter W. Lipman
U.S. Geological Survey, 345 Middlefield Road, Menlo Park, CA 94025, USA
e-mail: plipman@mojave.wr.usgs.gov

Introduction

Calderas associated with explosive ash-flow (ignimbrite) eruptions have been much studied during the past half century, stimulated by landmark reviews of caldera formation (Williams 1941) and ash-flow processes (Smith 1960), yet the processes of caldera formation and geometry of subsidence remain incompletely understood and controversial (McBirney 1990). Formation of ash-flow calderas by some form of roof collapse over an underlying shallow magma reservoir is now widely recognized as accompanying explosive eruptions that involve magmatic volumes greater than a few cubic kilometers. The term caldera, as used herein, includes features described in the literature as "cauldrons," which represent variably deeper erosional levels of the same fundamental structures and igneous processes.

In general, caldera diameter increases with volume of the associated ash-flow eruption. In their origin by subsidence, even small calderas are thus distinct from volcanic craters that form by constructional accumulation of cinders and spatter or by explosive ejection of wall rocks adjacent to a volcanic vent. Varied processes have been inferred as important or dominant: piece-

meal or chaotic subsidence (Williams 1941; Scandone 1990; Branney and Kokelaar 1994), plate (piston) subsidence of a relatively coherent floor bounded by ring faults (Clough et al. 1909; Smith and Bailey 1968); funnel-shaped subsidence into an areally restricted central vent (Yokoyama 1983, 1987, 1991; Aramaki 1984), and hinged downsag of a central area with little or no boundary faulting (Walker 1984; Branney 1995). Many individual calderas are geometrically complex, containing elements of more than a single structural type and subsidence process (Lipman 1984; Walker 1984; Branney 1995).

In addition to real diversity among caldera structures, the divergent interpretations of dominant subsidence processes reflect ambiguities resulting from the large dimensions of many calderas, incomplete cross-sectional exposures, overprinting by post-subsidence structures, and resulting uncertainties about subsidence geometries. Little-eroded young calderas with well-preserved eruptive morphology generally provide minimal information on underlying structures, depth of subsidence, or relation to the source magma reservoir. In contrast, where erosion has proceeded sufficiently to expose subvolcanic structures and granitic rocks of the solidified magma reservoir, the relations of such structures and intrusions to surface volcanic morphology commonly have been largely obscured. Complete sections from surface volcanic rocks to deep features of ash-flow calderas are preserved and exposed only rarely – in regions of exceptional topographic relief or sites of structural rotation of the upper crust.

Geometrically well constrained small-scale subsidence analogs, as in mine workings, nuclear-explosion craters, ice-melt pits, and experimental models, provide some insights into possible caldera geometries (Wisser 1927; Komuro 1987; Scandone 1990; Marti et al. 1994; Branney and Gilbert 1995). Although instructive, such analogs are difficult to compare rigorously with geometries and subsidence processes at large calderas, because the style of collapse likely depends strongly on rates of subsidence, aspect ratios and structural properties of roof rocks, and the presence or absence of a dynamic liquid substrate in the form of a silicate magma chamber. For example, studies of mine workings suggest that rapid subsidence causes the overlying ground to settle as a block, whereas gradual subsidence results in piecemeal adjustments of a jumble of fragments (Wisser 1927; Williams and McBirney 1979, p. 225). No natural caldera analogs are known to this author, however, that exemplify the second category: the cylindrical chaotic-collapse structures (chimney stopes) that are common in mine workings.

This overview proposes a generalized interpretive model for caldera-subsidence structures that form in conjunction with large-volume ash-flow eruptions, based largely on observations at well-exposed deeply eroded calderas. Structural elements and subsidence processes are reviewed for widely varying caldera types that have been carefully studied and well described, and these features are used to model subsidence geometry quantitatively for a few well-constrained calderas of widely varying sizes. Emphasis is on the effects of varying scales of volcanism, the role of intracaldera landslide breccias derived from unstable caldera walls, and contrasting shapes of the cogenetic subvolcanic magma chamber in relation to caldera-subsidence processes. Post-subsidence events, such as late caldera volcanism and resurgence, are not discussed. This summary amplifies and updates aspects of a previous synthesis (Lipman 1984) as well as assesses some divergent interpretations (e.g., Yokoyama 1983, 1987, 1991; Walker 1984; Aramaki 1984; Scandone 1990; Branney 1995). Many cited examples are from the western U.S. and Japan, but the resulting interpretations are considered broadly valid for other regions, volcanic types, and tectonic settings.

Caldera geometry: structural elements

Major structural and morphologic elements of a simplified caldera model (Fig. 1) include: topographic rim, inner topographic wall, bounding faults (if present), structural caldera floor, intracaldera fill (mainly ponded ash-flow tuff and landslide debris from caldera walls), and the underlying magma chamber or solidified pluton (Lipman 1984). Although highly generalized and not intended to accurately depict relations at any actual caldera, such a model provides a basis for discussing caldera structural elements and subsidence processes, computing approximate volumetric proportions between subsidence geometry and caldera-filling deposits (see Appendix), and inferring relations between eruption and subsidence processes.

Topographic rim

The topographic rim is simply the escarpment that bounds the subsided area of a caldera, beyond which lie largely undisturbed outer volcanic slopes. The rim encloses both the subsided area and also the area of scarp retreat due to rock falls and mass wasting. For young calderas, the topographic rim defines the overall areal extent of subsidence, although outlying circumferential fractures at some calderas accompany modest additional sagging toward the main subsided area. For eroded calderas, erosional mass wasting first tends to enlarge the original topographic rim, but later erosion of outer slopes of the upper caldera edifice can also reduce the apparent topographic diameter.

Inner topographic wall

The inner topographic wall is typically steepest in its upper parts, commonly as precipitous cliffs at young calderas, but tends to have a concave profile that flat-

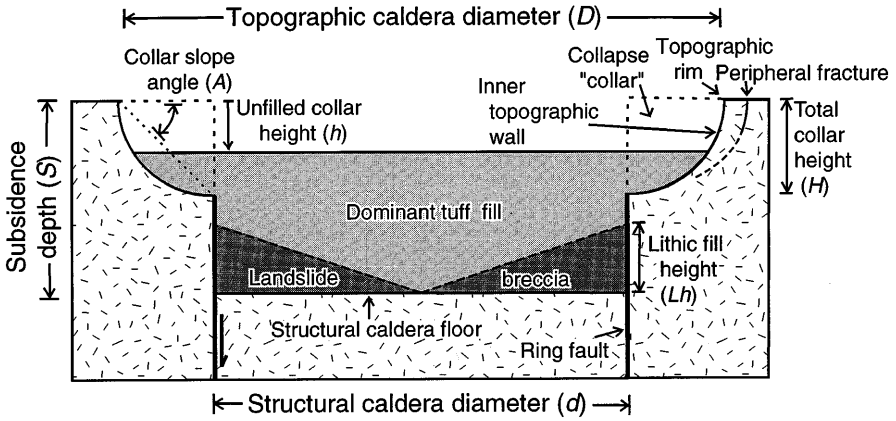

Fig. 1 Simplified model of plate (piston) caldera subsidence, showing geometric relations used in calculating the values in Table 1 and the Appendix. Ring faults, which typically dip steeply, are arbitrarily shown as vertical. The landslide breccia is shown schematically at the base of caldera fill, in order to permit geometrically simplified calculation of overall volume relations, rather than the more actualistic complex interfingering that occurs in many calderas. Presence of subcaldera magma chamber, any resurgent structures, and postcollapse volcanic constructs are omitted

tens down slope. Upper slopes of the inner topographic wall are virtually never an unmodified subsidence fault scarp; instead, they develop in response to landslide enlargement and rock falls from oversteepened slopes during and after caldera collapse. At the base of the topographically enlarged caldera wall, intracaldera fill may deposit directly against the caldera-boundary faults that have been unmodified by gravitational slumping. Such contacts are rarely likely to be preserved as depositional features, because continued caldera subsidence causes further faulting.

In plan view, the topographic walls of most large ash-flow calderas are scalloped by scarps of individual landslides and rock falls. Suggestions that topographic enlargement and the formation of scalloped embayments along some caldera walls result from irregular peripheral subsidence of overhangs along satellitic ring faults ((Branney and Gilbert 1995; Branney 1995, p. 314) may be valid for irregular walls of basaltic pit craters and other small collapse structures, but they are inconsistent with the structurally coherent bedrock stratigraphy that has been mapped along the footwall embayments in many large calderas, some projecting 5 km or more back from the main caldera wall (Steven and Lipman 1976; Yamamoto 1991; du Bray and Pallister 1991). Such shallowly rooted embayments can only have formed by surficial collapse and insliding along oversteepened caldera walls, an inference which is also documented by the provenance and large volume of slide material in adjacent caldera fill (Lipman 1976). Rarely, large scallops in walls of ash-flow calderas may be related to successive eccentrically overlapping subsidence events associated with recurrent eruptions (e.g., Toledo embayment of the Valles caldera; Self et al. 1986). At many multicyclic calderas, late large eruptions tend to cause subsidence of the entire prior caldera area, and earlier small subsidence structures tend to lie within the late caldera, e.g., Santorini in Greece (Druitt and Francaviglia 1992), Platoro in Colorado (Lipman et al. 1996).

Collapse collar

Material removed by mass wasting and scarp retreat defines a collapse collar (Fig. 1): the volume of rock lying between the topographic caldera wall and the structural caldera boundary. Average overall slopes of inner topographic walls (collar slope angle) are fairly gentle: 25° is typical, and 45° a probable upper limit. Lower slopes along the collapse collar, dipping as gently as 10–15°, are the only parts preserved in many eroded calderas, where the inner wall is expressed as an irregular unconformity between precaldera and caldera-filling rocks (Lipman 1976; Yamamoto 1992; du Bray and Pallister 1994). Gentle dips on lower slopes of the collapse collar permit exposure, by erosion or drilling, of precaldera rocks at shallow depths even at considerable distance inboard from the topographic rim. Such geometric relations have led to inference of funnel geometry for some large calderas (Yokoyama 1983, 1987; Aramaki 1984).

Bounding faults

Arcuate bounding faults (ring faults) are exposed at some deeply eroded calderas (mainly 5 km and greater in diameter), unambiguously defining plate (piston) subsidence, e.g., Bennett Lake in Canada (Lambert 1974), Lake City and Silverton in the western San Juan Mountains (Lipman 1976), Grizzly Peak in central Colorado (Fridrich et al. 1991), and many volcanic "cauldrons" and plutonic ring complexes in older terranes (summarized in Smith and Bailey 1968; Williams and McBirney 1979; Lipman 1984). Presence of bounding ring faults in some less eroded calderas can be inferred from the distribution of postcollapse vents, symmetrical resurgent uplift of caldera-filling volcanic rocks, and evidence for vents of the caldera-forming eruption along arcuate segments of caldera margins (Smith and Bailey 1968; Bacon 1983; Hildreth and Mahood 1986). The geometry of ring faulting in some eroded calderas

is more complex at deep levels, recording increasingly coherent plate collapse as the eruption progressed (Fridrich et al. 1991). Ring faults can accommodate uplift, as well as subsidence, e.g., domical magmatic resurgence at Lake City caldera in Colorado occurred along the same faults that had earlier accommodated caldera collapse (Hon 1987), and magma was injected as partial ring dikes. Similarly, trap-door uplift within the 45-ka Cinque Denti caldera in Pantelleria was accommodated by reversed movement along old ring fractures (Mahood and Hildreth 1986).

Ring faults that dip steeply inward at shallow crustal levels may steepen with depth and dip outward at levels just above the magma chamber into which the caldera subsided (Fig. 21 in Williams 1941; Branney 1995). In Figs. 1–3 all ring faults are arbitrarily shown as vertical. Some sizable calderas lack clear evidence for arcuate bounding faults (Walker 1984), but limited erosion depths typically preclude unambiguous interpretation. At many calderas regional tectonic trends have influenced the geometry of collapse to varying degrees (Komuro 1987; Ferguson et al. 1994; Rowley and Anderson 1996), but deeply eroded calderas bounded by strongly polygonal faults appear to be rare compared with those with arcuate fault boundaries.

Inference of a broad diffusely fractured structural boundary of subsidence (without large-displacement ring faults) that lies *outboard* of the topographic walls, based on analogy with small mine-subsidence and ice-melt-pit features (Fig. 6 in Branney 1995), has little support from exposed structures of deeply eroded ash-flow calderas that have been described thus far. Alternatively, circumferential extensional fractures peripheral to the topographic rims of young calderas are commonly associated with recurrent gravitational slumping of the free face of the inner caldera wall. Such peripheral fractures at Kilauea caldera in Hawaii have opened and closed repeatedly during major historical earthquakes, independently of caldera eruptive or subsidence events (Figs. 20–23 in Tilling et al. 1976).

Intracaldera fill

Intracaldera fill provides key evidence of caldera processes, because most or all large calderas collapsed during the associated eruptions, and ash-flow tuffs and interleaved caldera-wall slide breccias accumulated to multi-kilometer thickness within the subsided area (Lipman 1976). Distributions and volumes of slide breccia vs intracaldera tuff provide critical evidence on timing and geometry of subsidence.

In addition to tuffs and slide breccia that accumulated synchronously with caldera subsidence, most pre-Holocene calderas are partly to completely filled by younger lavas and tuffs erupted from postcollapse caldera-related vents, sedimentary debris eroded from adjacent volcanic highlands, and volcanic deposits derived from separate volcanic centers. Such postcaldera deposits tend to conceal the primary volcanic structures, especially at nonresurgent calderas, impeding interpretation of subsidence processes or even the presence of some large calderas. North American examples of large-volume caldera fills that postdate the climactic eruptive and subsidence event include the huge rhyolitic lava flows within the Yellowstone caldera, Wyoming (Christiansen 1984), the filling and overflowing of the nonresurgent South River caldera of the San Juan field by postcollapse andesitic lavas (Lipman et al. 1989), and the lacustrine sediments and interleaved lavas in La Primavera caldera, Mexico (Mahood 1980).

Caldera floor

The geometry of the structural caldera floor within the subsided area has been well documented at only a few large ash-flow calderas, and the typical degree of disruption during subsidence remains uncertain. The structural floor is the subsided precaldera land surface, in contrast to the topographic caldera floor exposed at the surface within a young caldera. Few calderas that are sufficiently preserved to provide a clear record of volcanic evolution are eroded to depths that expose their structural floors; in many, cogenetic magma has risen to such shallow depth that the floor has been destroyed. Subsidence structures at many deeply eroded calderas are complicated or obscured by multiple subsidence events associated with successive ash-flow eruptions or by later regional tectonism. Exceptional examples of structurally coherent caldera floors that subsided during a single large eruption are preserved in a few places where regional tectonic rotation has exposed calderas in cross section: for the western U.S., notably in the Stillwater Range, Nevada (John 1995), the eastern Sierra Nevada (Busby Spera 1984; Fiske and Tobisch 1994), Questa and Organ Mountains areas in New Mexico (Seager and McCurry 1988; Lipman 1988), and the Tucson Mountains in Arizona (Lipman 1993).

For many additional calderas, exposures of structurally coherent fill that accumulated within the caldera concurrently with subsidence provide strong evidence of at most limited disruption of the subsiding caldera interior. Even where the fill consists of massive tuff, the presence of partial cooling breaks, flow-unit partings, compositional boundaries, and interlayered landslide breccia sheets commonly provides stratigraphic markers to evaluate fault disruption within calderas; examples from the western U.S. are Timber Mountain (Carr and Quinlivan 1968), Organ Mountain (Seager and McCurry 1988), Lake City (Hon 1987), and Grizzly Peak (Fridrich et al. 1991). Most faulting of intracaldera fill that has been documented to date by such stratigraphic features occurred, not during subsidence, but during later resurgent doming or other uplift of the caldera floor, as indicated by displacement of all caldera-fill units. Intracaldera deposits are less well exposed in most nonresurgent calderas than they are on resurgent

blocks, but erosionally inverted topography at the nonresurgent Superstition Mountains caldera in Arizona (Sheridan 1978) and Chegem caldera in Russia (Lipman et al. 1993) provides exceptional exposures of widely continuous flow units and cooling breaks within thick exposed intracaldera tuff without significant fault disruption. Complex disruption of caldera floors may accompany overlapping subsidence during successive caldera-forming eruptions, but available evidence suggests to me that most large calderas subside fairly coherently during individual eruptions.

Growth faults, with upward decreasing displacement, should be present within syncollapse fill if the caldera floor were significantly disrupted during subsidence, but documented examples are rare. Because synsubsidence faulting would disrupt high-temperature tuffs as they welded, growth faults should be marked by conspicuous local rheomorphic zones, even where offset of lithologic markers was obscure. Documented examples of rheomorphic textures localized along faults that may have been active during subsidence include the Bachelor caldera in Colorado and the Tucson Mountains caldera in Arizona (Lipman 1984, 1993), but displacements are small relative to overall caldera subsidence. Widespread growth faulting has been well documented at the Ordovician Scafell caldera in England (Branney and Kokelaar 1994), but these faults variably displace multiple separate eruptive units, and relations to individual collapse events are less clear.

Small calderas (less than a few kilometers in diameter) merge in geometry with diatremes (Hearn 1966) and likely lack a coherent floor. Instead, the inner walls converge downward into the eruptive conduit in a funnel-shaped geometry, as discussed later.

Subcaldera magma chamber

Magma chambers, preserved as solidified plutons or batholiths, are exposed in many deeply eroded ash-flow calderas, as indicated by petrologic and age correlations with erupted volcanics. Such plutons have commonly been emplaced within a few kilometers of the regional volcanic surface, their roof zones protruding into the syneruptive fill of the associated caldera (summarized in Lipman 1984). Accumulation of silicic low-density magma in a large shallow chamber, which can generate uplift and tensile stresses at the surface, could be important in initiating ring faulting and permitting caldera collapse (Gudmundsson 1988; Marti et al. 1994). Such tumescence associated with growth of a subvolcanic magma chamber, which has been recorded instrumentally during many monitored eruptions and episodes of volcanic unrest, may be inadequate in magnitude to generate geologic structures that are detectable for prehistoric activity.

Shallow depths to incompletely solidified caldera-related magma chambers are documented for a few active calderas. Seismic-attenuation studies, magnetic curie-temperature depths, and other geophysical data indicate presence of magma at depths as shallow as 4–7 km at the 0.7-Ma Long Valley caldera in eastern California (Sanders 1984; Ponko and Sanders 1994; Steck and Prothero 1994; Sanders et al. 1995). Seismic-velocity structure has been interpreted as reflecting a hot granite body within approximately 2 km of the surface at the 0.6-Ma Yellowstone caldera in Wyoming (Eaton et al. 1975; Lehman et al. 1982; Iyer 1984; Smith and Braille 1994). Similarly, a low-velocity zone at 5–15 km depth is inferred to indicate the continued presence of melt beneath the 1.1-Ma Valles caldera in New Mexico (Ankeny et al 1986; Roberts et al. 1991; Steck et al., in press). At the historically active Rabaul caldera in Papua New Guinea, seismic hypocentral locations define an elliptical volume 5×10 km across; this volume is interpreted as bounded by ring faults overlying a central region of low seismicity at depths below 2–4 km that is inferred to represent the present-day magma chamber (Mori et al. 1989). For some older systems, the petrology of eruptive products also requires shallow depths of magmatic crystallization (e.g., presence of clinopyroxene rather than hornblende phenocrysts in most San Juan ash-flow sheets). Detailed inferences between shapes of exposed intrusions and collapse geometry are commonly ambiguous at eroded calderas, however, because subvolcanic magma bodies likely continue to evolve in composition, shape, and depth after cessation of the caldera-forming volcanism.

Despite such uncertainties, some consistent relations have emerged between collapse geometry and pluton shape. For example, several trap-door calderas in the western U.S. (Silverton, Bonanza, Mount Aetna, and Grizzly Peak in Colorado; Organ Mountains, New Mexico; Tucson Mountains, Arizona) expose high-level plutons along the most subsided side of an asymmetrical caldera, suggesting that maximum subsidence was influenced by the shallowest portion of the magma chamber. At several calderas high-resolution dating has documented cooling of subcaldera plutons within brief time intervals after caldera subsidence, e.g., at the Chegem caldera in southern Russia, $^{40}Ar/^{39}Ar$ mineral ages for eight samples of thin outflow tuff, thick intracaldera tuff, and intracaldera resurgent intrusion of porphyritic granodiorite are analytically indistinguishable at 2.82 ± 0.02 Ma (Gazis et al. 1995).

Several recent studies have inferred important roles for sills or shallow domical laccoliths of fine-grained hypabyssal rocks during caldera collapse (Gudmundsson 1988) and resurgence (Fridrich et al. 1991; du Bray and Pallister 1991), including introducing a special category of "laccocaldera" (Henry and Price 1989). Floors of such intrusions are generally not exposed, however, and their overall geometry remains uncertain. Other deeply eroded calderas expose large steep-sided subcaldera plutons containing granitic textures transitional to typical mesozonal batholithic bodies (Lipman 1984; Takahashi 1986; Johnson et al. 1989; Lipman et al. 1993; John 1994; Fiske and Tobisch 1994). Perhaps resurgent

intrusions initially spread as sill-like bodies near the base of the caldera fill, developing into stock-like plutons as continued emplacement of intrusive material gravitationally loads caldera-floor rocks and encourages block stoping, as proposed by Hon and Fridrich (1989). Any large caldera (>20 km diameter) must necessarily have been underlain by a batholithic-scale magma chamber of broadly tabular aspect ratio in order for the intrusion to reside in the middle and upper crust.

Caldera-subsidence processes

Prior approaches to subdividing and classifying calderas have tended to distinguish caldera types based on eruption style and magma composition at representative volcanoes, e.g., Krakatoan type, Valles type, Katmai type, etc. (Williams 1941; Macdonald 1972; Williams and McBirney 1979). Alternatively, the diversity of well-documented ash-flow calderas can be considered as a continuum of features and processes. Many calderas have such varied transitional geometries and structures that subclassification into discrete types seems less useful than relating subsidence geometry and resulting structures to a few geometrically simplified end-member processes.

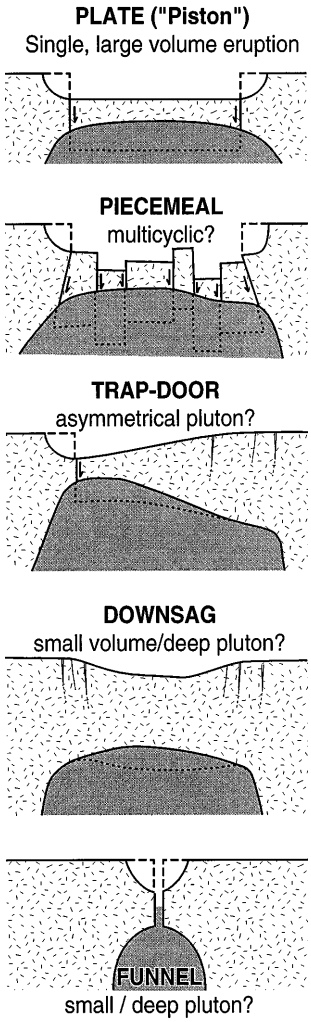

Fig. 2 Models of alternative subsidence geometries in relation to depth and roof geometry of underlying magma chamber. *Dashed lines* indicate postsubsidence depths of downdropped caldera floor blocks, which are inferred to have been partly removed by stopping into magma chamber during and immediately after caldera collapse

Size of the eruption and geometry of the cogenetic magma chamber also bear on subsidence processes. For example, stated distinctions between "Krakatoan" and "Valles" caldera types (foundering of the top of a composite volcano vs foundering independent of pre-existing volcanoes) are mainly functions of reservoir area and eruption volume, which influence resulting caldera size without any necessary difference in subsidence process. In the following discussion, five geometric end members (Fig. 2) are considered to encompass the broad variety of subsidence processes at ash-flow calderas. Many well-studied calderas involve subsidence processes intermediate between idealized end members. Ring-fault calderas can have complex boundaries involving more than a single arcuate bounding fault, both hinged downsag boundaries and ring faults are involved in trap-door caldera subsidence, and floors within some ring-fault calderas have sagged or faulted at loci where magma erupted rapidly (Lipman 1984; Branney 1995).

Plate subsidence

Many large calderas have long been recognized to involve plate (piston) subsidence of a relatively coherent floor, bounded by steeply dipping ring faults (Valles type; Smith and Bailey 1968). These calderas are associated with voluminous eruptions from large shallow magma chambers. The present author prefers the term *plate subsidence*, because for large calderas (>10 km diameter, especially resurgent ones) the diameter of the caldera floor must substantially exceed its thickness. At the Valles-type caldera, subsidence was followed by postcollapse domical uplift, but such resurgence occurs at only a small proportion of plate-subsidence calderas. Within most plate-subsidence calderas, the subsided lid over the source magma chamber is variably disrupted due to differential movement during ash-flow eruptions and postcollapse magmatism, but highly chaotic piecemeal subsidence has not been documented for any large-diameter calderas.

Ring and arcuate intrusions have long been recognized as deeply eroded analogs of large plate-subsidence calderas (Reynolds 1956; Buddington 1959; Smith and Bailey 1968). In the southern Rocky Mountains, ring faults are well exposed in the 13-×17-km Lake City and the 14-km Silverton calderas in the western San Juan Mountains (Steven and Lipman 1976), and at the 13-×27-km Mount Aetna and 17-×23-km

Grizzly Peak calderas in the Sawatch Range (Johnson et al. 1989; Fridrich et al. 1991). Many geometrically comparable plate-subsidence calderas, 10 km or more in diameter and bounded by ring faults, have been recognized recently in Japan, as Tertiary volcanic areas have been mapped geologically and explored by drilling (Yamada 1975; Ito et al. 1989; Yamamoto 1992a, 1994; Otake et al. 1997).

Some calderas as small as 4–5 km in topographic diameter appear to have fault-bounded floors, based on evidence for ring faults and structurally coherent caldera fill. Well-studied examples in the northwestern U.S. include the 4- × 6-km Holocene Crater Lake caldera (Bacon 1983; Nelson et al. 1994) and the 4.5- × 8-km Pleistocene Kulshan caldera (Hildreth 1996) in the Cascade Range. Several Tertiary calderas of similar size, containing evidence of plate (piston) subsidence, have recently been recognized in Japan, such as Ishizuchi in Shikotsu (Yoshida 1984), Haza and Masuda South in southern Honshu (Imaoka et al. 1988), Sanbe (Komuro et al. 1996), and Joko in the Aizu region of northern Honshu (Yamamoto 1994). Within the polycyclic Latera caldera in central Italy, the young 3- × 5-km Vepe caldera is interpreted "to involve coherent subsidence of a piston-like block" bounded by a ring-fracture system, based on the concentric distribution of postcollapse lava domes (Nappi et al. 1991).

Downsag subsidence

Large-scale downsag subsidence of ash-flow calderas has been inferred to be common, based on inward-sloping topography, inward-tilted wall rocks, and apparent absence of large-displacement ring faults at some major calderas (Walker 1984; Branney 1995). Many large plate-subsidence calderas involve subordinate downsag, but no deeply subsided calderas appear to have been well documented where downdropping is accommodated dominantly by inward tilting without major bounding faults, as is diagrammed as an alternative to ring-fault subsidence by Branney (1995, Figs. 3, 6).

Components of downsag, in conjunction with dominant subsidence along ring faults, appear to be common (Branney 1995) and include: (a) mild flexuring and fracturing during initiation of subsidence prior to establishment of a well-defined fault boundary, processes which accompany inception of all faulting of brittle upper crustal rocks; (b) incomplete ring-fault subsidence resulting in a hinged or trap-door caldera; (c) subordinate sagging of the structural caldera floor within bounding ring faults, as recognized for many years (Reynolds 1956); and (d) gravitationally induced inward late tilting and fracturing of oversteepened unstable caldera walls, in conjunction with slumping and landsliding. The appearance of downsag on the flanks of multicyclic caldera depressions can also be generated by volcanic units draped over a pre-existing caldera or structural basin:

1. Because most calderas resulting from large ash-flow eruptions subside several kilometers or more and are topographically enlarged by late slumping, clear evidence for initial flexuring and fracturing is rarely preserved. Precaldera volcanic rocks exposed along walls of young calderas mostly dip outward, rather than inward, and attitudes are compatible with primary volcanic dips or regional structural trends. Monoclinal flexures and extensional fractures probably accompany initiation of all ring faulting, as in regional tectonic faulting of brittle upper crustal rocks. Some inward-dipping fault-bounded slices, along the peripheries of a more intact central subsided area (e.g., Fig. 4F, G in Branney 1995), may represent such complexities inherited from initial stages of collapse that later was largely accommodated along ring faults. Other lenticular blocks tilted inward between master ring faults may mainly represent rotational drag during sustained subsidence.
2. Hinged (trap-door) subsidence is transitional between downsag and plate subsidence. At some calderas, inward-dipping rocks cited as evidence for downsag processes are likely the result of only modest overall vertical subsidence or the result of incomplete ring-fault subsidence, i.e., trap-door hinges as discussed in the next section.
3. Subordinate downsagging is common within caldera floors bounded by well-developed ring faults that accommodate the bulk of total subsidence. Saucer-like geometry of an otherwise coherent caldera floor may result from inward dips along the ring faults (Reynolds 1956), inheritance from broader downsagging during initial subsidence prior to full development of the bounding faults (Branney 1995), or generally from localized subsidence of the thermally weakened thin lid over a large shallow magma chamber as a result of focused magma drawdown during rapid eruption. Well-documented examples of downsagged caldera floors bounded by ring faults and ring dikes include Ossipee, New Hampshire (Kingsley 1931), Saboluka, Sudan (Almond 1977), and Ichizuchi, Japan (Yoshida 1984). The volume proportion of downwarping for some calderas (Ossipee, Glen Coe, Sabaloka) has been interpreted as approaching half of the recorded subsidence (Walker 1984; Branney 1995), but the actual proportion of downsag must be significantly smaller because the top of the basement (contact with base of outflow volcanics) is not preserved outside the subsided block at these ring structures.
4. Some large, coherently rotated, inward-dipping blocks along caldera walls are incipient slide blocks, related to second-order enlargement of the topographic caldera wall by landsliding, rather than primary collapse structures bounded by steeply dipping faults or fractures. One such partly detached block along the margin of the Chegem caldera in Russia is separated from the main caldera wall by a tuff- and breccia-filled fracture that is spectacularly exposed

for more than 300 m vertically (Lipman et al. 1993, p. 101). Some coherent slide blocks 1 km or more across have become stranded part way down the inner topographic wall of calderas (Lipman et al. 1989, p. 334; Fig. 10 in Yamamoto 1994), whereas others have been transported many kilometers into the caldera interior (Lipman 1976; Fiske and Tobisch 1994).

Of 30 examples cited by Branney (1995; Table 1) as "calderas with downsag," seven to nine have subordinate downsagging of caldera floors bounded by well-developed ring faults, and six are asymmetrical hinged trap-door calderas (as defined here) with incomplete ring faults. For two filled calderas with documented flanking downsags, Pine Canyon and Buckhorn in southwest Texas (Henry and Price 1984), erosional dissection is inadequate to evaluate the possible presence of concealed ring faults. Of the others, four are associated with recurrent incremental subsidence at basaltic lava calderas; downsag at six to eight are inferred from indirectly from surface morphology, or are open to alternative interpretations as discussed below, and several are based on unpublished data and are accordingly difficult to evaluate.

Inward-dipping foliations of intracaldera welded tuff that decrease in dip up section have been cited as evidence of downsag during eruption and subsidence at several calderas. In at least some cited examples (e.g., Lake City, Colorado, and Chegem, Russia, where this author has worked), however, such geometries are obvious results of differential primary depositional compaction of intracaldera tuff against caldera walls and caldera-margin slide breccias without need for any downsagging. At both these calderas deep glacially scoured canyons provide exceptional three-dimensional exposures of caldera-fill lithologies and geometry. Compaction dips are highly variable near caldera walls (locally approaching vertical), and tuff foliations correlate closely with adjacent buried slopes. Older volcanic strata in walls of these calderas dip horizontally or gently outward, and most prevolcanic strata are in continuity with regional structural attitudes –geometries incompatible with downsag as a dominant subsidence process.

Another inconclusive example of downsag subsidence is the Cerro Panizos caldera (15 km diameter) along the border between Bolivia and Argentina, which has been interpreted by Ort (1993) as having subsided weakly along a hinge-line marked by an inflection in dips of the volcanic strata. The main Cerro Panizos caldera, which formed during eruption of the lower cooling unit of the 6.7-Ma Panizos ignimbrite, is superbly preserved and exposed, but the limited erosional dissection precludes confident interpretation of its internal structure. On Ort's (1993) map, inward dips appear to be defined entirely by postcaldera tuffs (upper cooling unit) and overlying lavas. The main (lower) cooling unit dips outward but appears to have been overlapped by the inward-dipping younger tuffs and lavas, for which the relatively gentle inward dips (4–8°) could be entirely primary and compactional against buried inner slopes of the caldera.

Many basaltic lava-flow calderas (Hawaii, Galapagos, Olympus Mons, etc.) that have subsided repeatedly in small increments have an overall inward down-stepping geometry that has also been described as downsagged or downwarped (Walker 1988; Branney 1995). Such a geometry of nested sequential collapses within a single caldera during recurrent lava eruptions or intrusions along rift zones, although differing in scale from catastrophic caldera collapse during individual large explosive eruptions, may involve similar processes and be transitional to the multicyclic collapse histories that characterize many ash-flow calderas. In addition to small-scale incremental caldera collapse at basaltic volcanoes, at least some of these (e.g., Kilauea, Mauna Loa) also preserve evidence of longer-term cycles of caldera filling and recurrent collapse (Holcomb 1987; Decker 1987). Nested recurrent collapse events, although cumulatively generating an inward-sloping composite subsidence profile, need not involve any downsag during individual eruptions and caldera-subsidence events.

Although subsidence dominantly by downsag is not common at large ash-flow calderas, a component of downsagging and extensional fracturing is associated with many developing ring faults. Downsag processes may be most important where subsidence is incomplete or relatively shallow and may be favored by deeper magma chambers or smaller eruptive volumes.

Trap-door subsidence

Trap-door subsidence, bounded by a partial ring fault and by a hinged segment, constitutes incomplete or incipient plate collapse; as such, it is intermediate between plate and downsag subsidence processes. Such partial subsidence may be related to smaller eruptions, an asymmetrical magma chamber, or regional tectonic influences. Geometrically well-defined examples of trap-door subsidence in the western U.S. include Silverton, Bonanza, and Mt. Aetna calderas in Colorado (Steven and Lipman 1976; Varga and Smith 1984; Johnson et al. 1989), the Organ Mountains caldera in New Mexico (Seager and McCurry 1988), Eagle Mountain caldera in Trans-Pecos, Texas (Henry and Price 1984), Three Creeks and Big John calderas in Utah (Steven et al. 1984), Pueblo and Whitehorse calderas along the Oregon–Nevada state line (Rytuba and McKee 1984), and the Tucson Mountains caldera in Arizona (Lipman 1993). Well-described hinged or trap-door calderas elsewhere include Snowdon caldera in Wales (Howells et al. 1986), Bolsena in central Italy (Nappi et al. 1991), and Sakugi in southwest Japan (Murakami and Komuro 1993).

The Tucson Mountains caldera, source of the 72-Ma Cat Mountain tuff, is particularly instructive, because

postvolcanic tectonic rotation in the upper plate of a regional detachment fault has provided cross-sectional exposures completely through the caldera-fill section. The intracaldera Cat Mountain tuff is lithic poor and only approximately 100 m thick at the hinged southern margin of the caldera, but the caldera fill thickens gradually to a thickness of 4–5 km at the most downfaulted opposing margin. Along this margin, the bulk of the caldera-fill material consists of collapse breccia derived from the caldera walls, interfingering with discontinuous matrix of ash-flow tuff.

Piecemeal disruption

Small-displacement piecemeal faulting of subsiding caldera floors is probably common. Fracturing during subsidence has been documented for a few calderas by growth-fault deformation of an intracaldera tuff unit concurrently with welding (e.g., Fig. 8 in Lipman 1984; Fig. 9 in Branney and Kokelaar 1994). Complex piecemeal fracturing of caldera floors on a coarse scale, bounded by arcuate or rectilinear growth faults, has been interpreted as the dominant subsidence process for a few calderas (Branney and Kokelaar 1994). Such features can result from interaction with the prevolcanic structural grain or from intricate fracturing of the caldera floor during a single eruption.

Without clear evidence of large-scale growth faulting during a single eruption, piecemeal fracturing of a caldera floor is open to alternative interpretations. Geometrically complex fracturing should be expected at sites of multiple nested or overlapping collapses that cause incremental subsidence during successive ash-flow eruptions, as is likely present in floors of overlapping caldera complexes that subsided recurrently at intervals of tens to hundreds of thousand years, such as in the San Juan Mountains of Colorado (Lipman et al. 1996), calderas of the southwest Nevada volcanic field (Christiansen et al. 1977; Sawyer et al. 1994), Bolsena and Latera calderas in central Italy (Nappi et al. 1991), and the Kagoshima Bay area of southern Japan (Matumoto 1943; Aramaki 1984; Nagaoka 1988).

Similar complexities in caldera-floor geometry may also be indicated by scattered or transverse distributions of postcaldera postcollapse vents within recurrently subsided calderas, as at Campi Flegrei, Aso, or Santorini (Walker 1984). Analogous complexities in subsidence geometry appear to be present at the historically active Rabaul caldera in Papua New Guinea, where geologic relations document successive overlapping caldera subsidences during the past few hundred thousand years (Nairn et al. 1995), even though present-day seismicity defines a geometrically simple ring-structure boundary for the active caldera (Mori et al. 1989).

Interpretation of the carefully studied Ordovician Scafell caldera in the English Lake District as a piecemeal subsidence structure (Branney and Kokelaar 1994) is dependent on inference of subsidence along growth faults during a single eruption, but the multiple intracaldera depositional units that have been mapped appear to record diverse eruption and emplacement processes during accumulation of the intracaldera fill. The complex fill stratigraphy at Scafell differs from that typical of accumulations during single eruptive cycles at younger calderas and suggests alternatively that subsidence was incremental during successive eruptions over a sustained time interval.

Chaotic subsidence

Chaotic subsidence, marked by intense wholesale disruption and brecciation of caldera-floor rocks, has been inferred to be an important caldera-forming process in some reviews (Fig. 37 in Williams 1941; Yokoyama 1983; Fig. 14 in Scandone 1990), but such processes are not documented by features of any deeply eroded large ash-flow calderas known to this author. Chaotic subsidence has been proposed as a process to generate (a) low-density material within calderas that can account for the observed negative gravity anomalies (Yokoyama 1983, 1987), and (b) lithic breccias by collapse of the roof over a depressurizing magma chamber (Fig. 14 in Scandone 1990). As discussed below, however, observed gravity anomalies in calderas can be modeled successfully with alternative assumptions, and voluminous lithic breccias within many calderas are demonstrably formed by gravitational failure and landsliding of oversteepened walls adjacent to ring faults. Thick megabreccias exposed in deeply eroded calderas typically are interleaved conformably with ash-flow tuff, indicating that such breccias are depositional units of the caldera fill (Lipman 1976; Hon 1987; Fridrich et al. 1991; Fiske and Tobisch 1994; Yamamoto 1994) rather than drastically disrupted floor. Large landslides from the inner caldera walls (the collapse collar volume) are also a potential source of voluminous lithic material, in addition to direct vent erosion, that could be entrained in the eruption column and emplaced as lithic lag breccia; chaotic disruption of floor or vent material (Walker 1985; Scandone 1990; Rosi et al. 1996) need not be the sole or even dominant source. The volumes of lithic lag breccia in proximal outflow deposits are typically small in comparison with the slide breccias that accumulate within the subsided area.

Funnel calderas

As pointed out by Branney (1995, p. 316), the term funnel-shaped is potentially ambiguous for caldera structures. In this review virtually all calderas are considered to be funnel-shaped in overall geometry, in the sense that their topographic walls flare outward from the structural boundaries, due to gravitational slumping (Figs. 1, 2). A funnel-shaped structural boundary can

also result from severe downsag, piecemeal subsidence, or probably more commonly from recurrent subsidence during successive eruptions. Alternatively, some calderas, especially in Japan, have been interpreted as structural funnels due to upward flaring of the primary eruption conduit (Yokoyama 1983, 1987; Aramaki 1984). The following discussion focuses on the scale of such structural–funnel subsidences.

Small calderas (<2–4 km diameter at topographic rim) commonly have a funnel geometry, because enlargement by slumping of the inner wall into an areally restricted vent is the dominant process in establishing the overall size of the subsided area. Such calderas are associated with explosive eruptions from a central vent, lack a bounding ring fault or a coherent subsided block, and probably overlie relatively small (and deep?) magma chambers. Well-documented funnel calderas, associated with relatively small-volume ash-flow eruptions, include Nigorikawa and Sunagohara calderas in northern Honshu, Japan, which are especially well constrained in three dimensions by geothermal drilling (Ando 1981; Dohnan Geothermal Energy Co. 1984; Yamamoto 1992b; Mizugaki 1993), Red Hills, Utah (Cunningham and Steven 1979), and the Novarupta vent that formed during the 1912 Katmai eruption in Alaska (Eichelberger and Hildreth 1986; Hildreth 1987). Such funnel calderas appear to merge in geometry and structural type with diatremes associated with explosive eruption of more mafic magma to form tuff rings and maars (Hearn 1966).

Small funnel calderas have not been widely recognized in eroded Tertiary volcanic areas, in part because the sources of ash-flow sheets smaller than 10–20 km^3 tend to be overwhelmed and obscured by larger tuff eruptions. For example, some small ash-flow sheets erupted from the Platoro caldera complex in the San Juan field (Middle tuff: ten or more sheets with individual volumes of 5–10 km^3; Dungan et al. 1989) may have been associated with small funnel calderas that were subsequently displaced downward and concealed during later larger-volume eruptions. As suggested by G. P. L. Walker (pers. commun.), several of the well-known British Tertiary centers contain breccia masses several kilometers in diameter that could be small funnel calderas. These breccias were studied when knowledge of brecciation process in volcanic settings was rudimentary and originally were interpreted as intrusions, but several involve subsidence of debris from higher levels. Possible candidates for small funnel calderas include: the Loch na Creitheach vent at Skye, breccias cropping out along the Slieve Gullion ring dike, and "explosion" breccias that are exposed over a 3-×9-km area along the margin of the early caldera on Mull (described in Emeleus and Gyopari 1992).

Some large young calderas, especially in Japan, have been inferred to have a funnel shape, based mainly on modeling of gravity anomalies (Yokoyama 1983, 1987, 1991). Such funnel structures have been inferred to develop in relatively weak crusts of young island arcs, in contrast to ring-fault and plate-subsidence of calderas in cratonic environments (Walker 1984; Scandone 1990). In contrast, no large funnel structures have been documented for eroded calderas in Japan, even though many ring-fault calderas and plate-subsidence structures have recently been recognized in eroded Tertiary volcanic fields (Yamada 1975; Sawada 1984; Yoshida 1984; Takahashi 1986; Takada 1987; Imaoka et al. 1988; Ito et al. 1989; Yamamoto 1992a, 1994; Otake et al. 1997; Miura 1997).

Proposed distinctions between caldera types in Japan as a function of regional tectonic stress field, relating the Tertiary plate-subsidence calderas to periods of extension and funnel structures to more recent arc-normal compression (Sawada 1984; Yoshida 1984), also seem unconvincing. Several carefully studied Pleistocene calderas in southern Japan that have been interpreted as representative funnel structures are associated with broad zones of normal faulting and graben structures, including Aira and other calderas in Kagoshima Bay (Aramaki 1984; Yokoyama and Ohkawa 1986) and the Shishimuta caldera in northeastern Kyushu (Kamata 1989). Clusters of ash-flow calderas along arc-related graben are also conspicuous in other arc systems (e.g., Toba in Indonesia, Taupo in New Zealand, intra-arc graben of Central America).

A further complexity for large calderas inferred to have funnel geometry is the ambiguity of interpretations based on gravity data. A plate subsidence structure with lithic debris concentrated near structural margins, as is commonly observed in eroded calderas, can generate a gravity profile indistinguishable from a funnel structure. Some Japanese calderas, interpreted as having negative Bouguer gravity profiles indicative of funnel structure, have steep-sided U-shaped gravity anomalies that could alternatively be modeled as small ring-fault subsidence structures, e.g., Shishimuta caldera in Kyushu (Kamata 1989). Geometrically simplistic gravity modeling of other Japanese calderas as funnel shaped (e.g., Aso caldera; Yokoyama 1983) is complicated by recurrent eruption of multiple large ash-flow sheets and multi-stage incremental subsidence. Recent detailed processing of gravity data for Aso suggests multiple flat-bottomed gravity lows and an overall "piston-cylinder type structure rather than a funnel-shaped structure" (Komazawa 1995). Elsewhere, deep erosional exposure and/or exploration drilling has documented that an overall funnel-like geometry can result at large ash-flow calderas from multi-stage subsidence along nested ring fractures (Halliman 1993; Lipman et al. 1996).

Ignimbrite "shields"

While caldera sources have been identified worldwide for most well-preserved large ash-flow sheets, among the late Tertiary volcanoes spectacularly exposed on the altiplano of the central Andes are silicic centers

where a large-volume tuff sheet dips gently outward from a central lava dome complex. Initially interpreted mainly from satellite images for this difficult-to-access, high-altitude region, these have been described as ignimbrite "shields" that erupted without significant caldera collapse or resurgence (Baker 1981; Francis et al. 1984; de Silva and Francis 1991). Ignimbrite shields have been proposed as an important but little-recognized class of explosive silicic centers that reflect eruption from relatively deep magma chambers (de Silva 1997).

Because Andean volcanologists have also described many plate-subsidence and resurgent calderas and noted their similarities to ash-flow centers in North America (Sparks et al. 1987; Gardeweg and Ramirez 1987; de Silva 1989), the apparent absence of comparable ignimbrite shields in the western U.S. suggests the possibility of interpretive problems with the Andean ignimbrite "shields" resulting from their lack of dissection, inaccessibility, and resulting limited field study. At least some ignimbrite shields seem alternatively interpretable as conventional (structurally bounded) nonresurgent calderas, surrounded by their ignimbrite aprons, that were filled to overflowing by younger intracaldera lavas and tuffs.

Potentially analogous nonresurgent large calderas that were once completely buried by later volcanic deposits have been exposed by erosion in the western U.S. For example, at least five large San Juan calderas (Silverton, San Luis 1 and 2, Lost Lakes, South River) failed to resurge but instead were filled by lava and tuff erupted from within the subsided area prior to the next major ash-flow cycle. Some intracaldera and caldera-margin constructs in the San Juan region were stratovolcanoes originally rising thousands of meters above the regional terrain; others were clusters of smaller lava domes that interleave with pyroclastic-flow and volcaniclastic sedimentary deposits. The primary pre-erosion morphology of filled calderas in the Rocky Mountains would have looked strikingly like the described ignimbrite shields of the Andes. In comparison with the altiplano region, and its superb exposures of near-pristine unvegetated volcanic features, the Southern Rocky Mountains provide the advantage of exposing a third dimension in glacial canyons 1 km or more deep (along with disadvantages such as heavy vegetation).

Ground-based field studies at several silicic centers in the Andes that were initially interpreted as ignimbrite shields from satellite images have yielded alternative caldera interpretations. The Morococala volcanic field in Bolivia was originally interpreted as a single ignimbrite shield approximately 30×60 km across (Baker 1981), but subsequent reconnaissance mapping has identified three ash-flow sheets, emplaced at 8.4, 6.8, and 6.4 Ma, that are interpreted as erupted from two discrete ring-fault bounded calderas, within which late-erupted tuff ponded during subsidence (Luedke et al. 1990). The Cerro Panizos area along the Bolivia–Argentina border was also initially interpreted as an ignimbrite shield approximately 40 km in diameter that experienced little or no collapse (Baker 1981), but field studies (Ort 1993) suggest the presence of two nested caldera subsidences largely inundated by lava flows and domes. The first caldera was interpreted by Ort as a downsag structure, but as discussed previously, this 15-km-diameter depression may alternatively be fault bounded, with later-erupted ash-flow tuffs and lavas ponded unconformably against the inner caldera walls.

Volcano-tectonic depressions

Inferred sources for some large ash-flow eruptions, interpreted to have vented directly from regional graben without developing localized calderas, have been described as volcano-tectonic depressions (e.g., Macdonald 1972, pp 312–313; Williams and McBirney 1979, pp 226–228). While ash-flow eruptions and associated calderas have long been recognized as associated with extension tectonics, no large pyroclastic eruptions have been shown to be accompanied mainly by subsidence along regional graben. Many typical subequant calderas are known within and adjacent to major graben and rift zones; examples include the Valles and Questa calderas along the Rio Grande rift in northern New Mexico (Smith and Bailey 1968; Lipman 1988), Long Valley caldera in Owens Valley along the west side of the Basin-Range Province in eastern California (Bailey 1976), calderas of the Yellowstone system along the Snake River plain in southern Idaho (Christiansen 1984; Pierce and Morgan 1992), and Permian calderas of the Oslo graben (Oftedahl 1978). While the margins of many subequant calderas are influenced by regional structures, some developing polygonal fault boundaries (Komura 1987; Rowley and Anderson 1996), drastic elongation of individual ash-flow subsidence structures along regional structural trends seems rare. To the contrary, some calderas along regional graben are elongate perpendicular to their graben setting, e.g., Long Valley, Questa.

Association of ash-flow eruptions and caldera formation with regional extension leads to subsidence and burial of calderas along axes of graben, obscuring relations between volcanism and tectonic setting. Increasingly, more detailed geologic, geophysical, and deep-drilling data have demonstrated that several regions commonly cited as volcano-tectonic depressions contain clusters of subequant calderas along the graben axis. Examples include the Taupo graben in New Zealand, where at least eight major ash-flow calderas that have formed since 2 Ma are variably concealed beneath volcanic and sedimentary fill (Wilson et al. 1984; Nairn et al. 1994); the Toba depression in Indonesia, where four discrete ash-flow eruptions were accompanied by caldera collapses from varying locations between 1.2 Ma and 75 ka (Chesner and Rose 1991); and Kagoshima Bay in Japan, where at least five calderas have

erupted in the past million years (Aramaki 1984; Nagaoka 1988). Even where bounding caldera faults consist of linear segments, the surface expression of caldera subsidence typically assumes a more nearly circular geometry as unsupported oversteepened walls slump into the central depression. On a smaller scale, even the strongest linear extensional structures can host circular volcanic subsidences, as exemplified by the development of equant pit craters along rift zones of Hawaiian volcanoes.

Geometry of subsidence: examples and models

A simplified geometric model for calderas of widely varying size and structural type, whose dimensions are relatively well constrained (Figs. 1, 3, 4), permits approximate calculation of caldera-fill volumes and subsidence depths that can only rarely be observed directly (Table 1; see Appendix) This analysis also illustrates the important volumetric role of gravitational landslide enlargement of caldera walls in determining overall caldera size, contributing to the lithologic diversity of the intracaldera fill, and resulting stratigraphic and geophysical interpretive complexities. Although the model utilizes simple plate subsidence of the caldera floor for ease of volume calculations, more complex subsidence processes (hinged, piecemeal, chaotic) would not substantially modify the conclusions. Key dimensions used in the calculations, and associated uncertainties, are summarized briefly.

For many calderas, the *topographic diameter* is well defined, and the *structural diameter* can be inferred from distribution of postcollapse vents and/or shape of resurgent uplift (Fig. 7 in Lipman 1984); from these, dimensions of the *collapse collar,* related to landsliding of the unstable inner wall, also can be determined, permitting calculation of the volume of wall rock that must either accumulate within the subsided caldera area as landslide debris or be expelled explosively as lithic debris in the ash flows.

Unfilled collar height above the topographic caldera floor commonly is observable directly. *Total collar height* is more approximate, because caldera fill commonly extends into the collar area, but can be projected if the structural boundary of the subsided area can be determined or inferred. Parts of the inner caldera walls are exposed at many calderas, both young and old, but the overall slope of the inner wall (*collar slope angle*) is virtually never preserved over its entire vertical extent; accordingly, an average angle is used for the model interpretations. The *collar volume* can be approximated using an average slope of the inner caldera wall, or more rigorously by a geometrically more complex concave-upward profile such as characterizes actual caldera walls. The planar-wall simplification underestimates the volume of the collar and the wall-rock material available to generate lithic debris; for a collar as high as its horizontal extent, a curved profile could add as much as 60% additional volume.

The collar volume and overall volume of caldera subsidence are virtually impossible to determine with accuracy. The configuration of the presubsidence surface (volcanic constructs, previous caldera basins, etc.) is known only for a few small historical calderas, and the geometry of the buried caldera floor is ambiguous for pristine young calderas. For eroded calderas, secular erosive retreat of the caldera wall can be an additional complexity in estimating the collar volume. Such erosion reduces the unfilled collar height and initially enlarges the topographic rim, geometric effects that would tend to have counterbalancing effects on collar volume. Sustained erosion that removes upper parts of the topographic wall reduces the apparent area of the topographic caldera, diminishing the apparent collar volume. Erosion of the inner walls appears to be a subordinate process in the filling of most caldera depressions, however; primary postcollapse volcanic deposits (lavas and tuffs) tend to dominate greatly over volcaniclastic sediments.

The distribution of *intracaldera landslide breccia* in relation to tuff fill is shown schematically as a debris fan at the base of all the intracaldera fill in Fig. 1. This simplification is used rather than a more actualistic interfingering, in order to permit geometrically simplified calculation of overall volume relations; the important parameter is the proportion of slide breccia vs intracaldera tuff, in relation to the collar volume. Exposures in many eroded calderas in North America and Japan demonstrate that slide debris interfingers complexly with

Table 1 Dimensions of key caldera elements and calculated volumes of intracaldera fill for a range of caldera sizes, based on a simplified geometric model (Figure 1). See Appendix 1 for complete listing of model calculations and equations

Dimension (km)	Nikorikawa (funnel)	Aira		Crater Lake (ring fault)	Creede (ring fault)	La Garita (ring fault)
		("funnel")	(ring fault)			
Diameter (topographic)	2.5	20	20	9	24	50
Diameter (structural)	(0.5)	6±	12	5	14	40
Collar, unfilled height	0.2	0.3	0.3	1	1.5	1.5
Collar volume (lithics)	2.7	235	84	20	270	680
Subsidence depth	6	4	4	3	4.5	4
Tuff fill volume (km^3)	0.3	28	363	19	205	2500
Lithic fill (%)	90	89	34	51	57	21

concurrently deposited intracaldera tuff but tends to accumulate as debris fans adjacent to margins of the subsided block, with only modest slide debris reaching central parts of the caldera (Lambert 1974; Lipman 1976; Hon 1987; Yamamoto 1991, 1992, 1994; Fridrich et al. 1991; Hildreth 1996; Otake et al. 1997). Such a configuration can approximate the geometry of a gently dipping funnel boundary between dominant tuff fill and redeposited wall-rock material, even in calderas with well-defined ring faults and plate subsidence (e.g., Bennett Lake, Lake City, Grizzly Peak calderas). Intracaldera tuff is typically present only locally between megabreccia clasts, and it is commonly nonwelded owing to chilling by cold clasts. Because such landslide breccias can contain individual megaclasts hundreds of meters across, distinction between slide debris and in-place wall (or floor) rock can be difficult, even in surface exposures. In drill core or cuttings, such distinctions may not be feasible.

Some wall-rock material disrupted by collar enlargement escapes from the caldera as lithic fragments in the ash flows. Large-volume ash flows typically contain fewer lithic fragments than do some small tuff sheets, indicating increasing eruptive efficiency with eruptive scale. Ash-flow sheets having volumes of 50–500 km^3 rarely contain more than a few percent lithic clasts overall: lithic lag breccias (Walker 1985) can be conspicuous in proximal exposures but are volumetrically minor overall components. For the examples discussed herein, in comparison with the planar-slope simplification used in model calculations, the additional lithic volume implicit in an actualistic concave inner wall geometry is probably adequate to account for the lithic volume removed from the caldera by the ash flows.

Total *subsidence depth* is rarely directly observable for large ash-flow calderas, but a minimum value is the sum of the unfilled collar height plus exposed caldera-fill thickness. Many deeply eroded large calderas expose several kilometers of syneruptive fill, and some sections through tilted calderas show fill thicknesses of as much as 3–5 km, e.g., Questa (Lipman 1988), Organ (Seager and McCurry 1988), Stillwater Range (John 1994), Tucson Mountains (Lipman 1993). For the calderas modeled below, ranges of subsidence depths and other parameters were used to calculate alternative solutions (see Appendix). Where not otherwise constrained, values were selected to match or exceed the minimum subsidence depth that would accommodate the *lithic-fill height* of landslide debris inferred to have accumulated within the structurally bounded caldera. The best solutions for total subsidence depths at large ash-flow calderas are typically at least 3–4 km, far thicker than most naturally exposed sections of intracaldera deposits.

For computational simplicity, the caldera floor is shown as an unbroken subsided plate in Fig. 3, but the geometric calculations would be little changed if more piecemeal subsidence were involved. Some caldera floors have sagged into a basin shape during subsidence, due to influences of inward-dipping ring faults (Reynolds 1956) or of other more complex geometries (Branney 1995). In such calderas the subsidence depth necessarily decreases toward the structural margins, a complexity ignored in the geometrically simplified models of Figs. 1 and 3. The presence of a downsagged floor would reduce the caldera subsidence volumes computed for any maximum subsidence depth in Table 1 and the Appendix. Because the volume of intracaldera lithic debris is constrained by the collar volume, not subsidence depth, the proportion of lithic debris to intracaldera tuff would increase for calderas with basin-shaped floors.

For small funnel-shaped calderas, such as Nigorikawa, the computed lithic-fill heights are implausibly large (see Appendix). For such structure much of the intracaldera lithic debris accumulates within the funnel above the small-diameter vent pipe, analogous to accumulation in the collar beyond the structural boundary of larger ring-fault calderas.

Observed values for these parameters, and estimated values for those not directly measurable, have been applied to varied caldera sizes and geometries. Preferred solutions for a few are listed in Table 1 and illustrated in Fig. 3; some alternative spreadsheet calculations and the equations utilized are listed in the Appendix. Summarized below are assumptions, alternative solutions, and volcanologic implications:

Nigorikawa

The late Pleistocene Nigorikawa caldera is a representative small funnel subsidence structure in southwestern Hokkaido, Japan, which is especially well understood because of geothermal exploration drilling to depths of 2.6 km (Ando 1981; Dohnan Geothermal Energy Co. 1984). Inward slopes of the funnel are steeper than typical of larger calderas, averaging more than 50°, and probably reflect rapid filling during a relatively small-volume eruption. The funnel is described as filled by pyroclastic breccia, but detailed descriptions of the proportions of tuff and lithics are unavailable. In terms of the caldera model developed here, small funnel calderas such as Nigorikawa are dominated by collar enlargement, without a coherently subsided central block. In any reasonable geometric solution (Fig. 3A; see Appendix), the volume of wall rocks derived from the collar suggests subsidence of lithic material to depths of at least 4–6 km, well within the vent pipe, even with only minor admixed tuff. Lithic material is comparably transported downward in deeply eroded diatremes (Hearn 1966). The structural diameter of the vent is constrained by the drilling results as no larger than approximately 0.5 km in diameter; if smaller, the modeled depth reached by lithic material from the funnel-shaped collar would be even greater. Because much of the associated outflow tuff sheet has entered the ocean, its original volume and lithic content are poorly con-

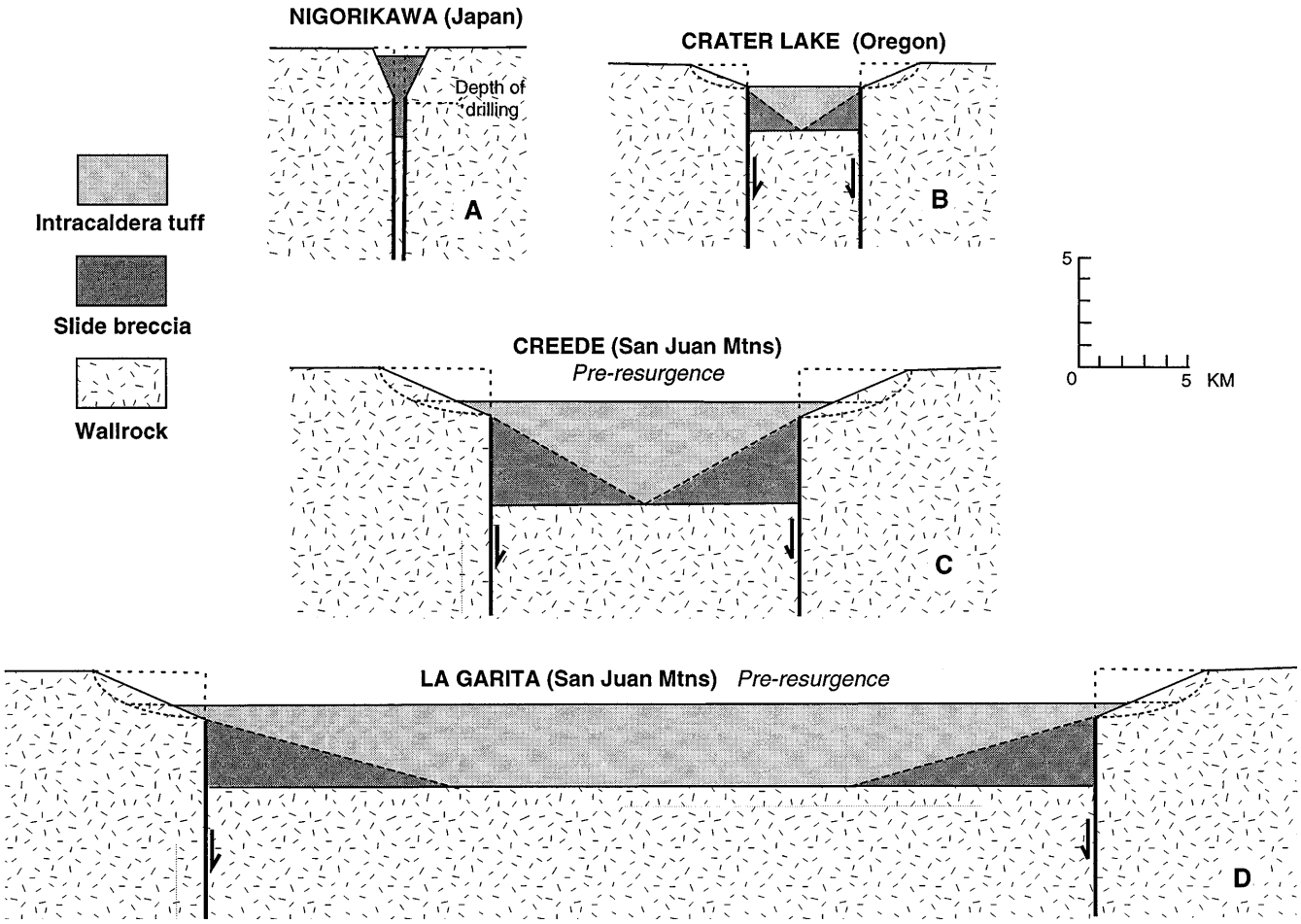

Fig. 3 Simplified scaled dimensions of four geometrically well-constrained calderas, based on generalized model of Fig. 1. Diagrams illustrate computed proportions of ash-flow tuff and slide breccia in caldera fill (see text for discussion of assumptions, Table 1 for observed dimensions and calculated parameters). The landslide breccia is shown at the base of caldera fill and the caldera floor as a simplified planar surface, in order to facilitate calculation of overall volume relations, rather than the more actualistic complex interfingering of fill and more complex floor geometry that occurs in many calderas. Inner caldera walls are modeled as a planar cone segment for volume calculations. Presence of subcaldera magma chamber and postcollapse volcanic constructs are omitted. Occurrence of water at Crater Lake and postcollapse resurgence at Creede are neglected. **A** Nigorikawa, Japan: funnel-shaped caldera. **B** Crater Lake, Oregon: small plate-subsidence caldera. **C** Creede, Colorado: average plate-subsidence caldera. **D** La Garita, Colorado: large plate-subsidence caldera

strained (S. Aramaki and T. Ui, pers. commun.). Comparison with young calderas of similar diameter suggests an outflow volume of only a few cubic kilometers, in which case even abundant lithic clasts (10–15%) could account for at most a small fraction of the 2.7 km^3 collar volume. Thus, at small funnel calderas, the volume of lithic material generated by vent enlargement and inward sliding likely dominates the intracaldera fill.

Crater Lake

Crater Lake, site of the 6800 radiocarbon years B.P. eruption of Mazama ash and the focus of pioneering caldera studies by Williams (1942), is a representative mid-size caldera. Ash-flow eruptions and caldera collapse are interpreted to have been dominantly along an elliptical ring-fracture zone with an average diameter of approximately 5 km (Bacon 1983; Nelson et al. 1994). Fill of the caldera by 600 m of water to a level 300–400 m below the topographic rim provides a minimum of 1 km collar depth (Fig. 3B). Bathymetric and submersible observations indicate the presence of several postcollapse andesitic volcanoes on the lake bottom, in addition to tuff and sediments that ponded within the caldera during subsidence concurrently with and subsequent to the climactic eruption (Bacon 1983; Nelson et al. 1994). Total subsidence is estimated to have been greater than 2.5 km, based on the height of a slide-debris fan within the subsided block needed to account for the collar volume (20 km^3, assuming a simplified planar inner caldera slope). The volume of lithic material in the outflow tuff sheet, as much as 6–10 km^3 (Bacon 1983; C. R. Bacon, pers. commun.), is comparable to likely amounts of additional debris that would result from a more actualistic concave-upward inner caldera wall, rather than the simplified planar model

geometry. The volume and nature of juvenile intracaldera tuff are uncertain; the preferred model calculation of 20 km^3 would constitute approximately one third of the total magma erupted during caldera formation.

Creede

The 24-km-diameter Creede caldera is thought to be a representative medium-size plate-subsidence caldera (Steven and Lipman 1976), similar in size and overall geometry to other well-studied resurgent calderas in the western U.S. such as Valles (New Mexico), Timber Mountain (Nevada), and Long Valley (California). Creede caldera, which formed during eruption of the Snowshoe Mountain tuff at 26.5 Ma, is the best-preserved caldera in the central San Juan field. Although not directly exposed, a ring fault approximately 14 km in diameter is inferred from arcuate trends of postcollapse lava vents and fossil hot-spring deposits, as well as from strong resurgent doming along confocal boundaries (Steven and Lipman 1976). Drilling in the caldera moat (Bethke et al. 1994) has penetrated the top of flat-lying intracaldera tuff at a depth of 1.5 km below the caldera topographic rim, providing tight constraints on the original "unfilled collar height" (partly filled by postcaldera sediments and lavas). The presence of intracaldera tuff in drill holes beyond the structural margin demonstrates overlap of this tuff onto the inner caldera wall (Fig. 3C). Intracaldera tuff at least 1.8 km thick crops out on the resurgent dome without any exposures reaching its base. Thus, the combined 3.3 km of unfilled collar depth and exposed intracaldera tuff is a minimum subsidence depth. Because only volumetrically minor landslide breccias interleave with tuff exposed on the resurgent dome near the center of the caldera, the large collar volume indicates that catastrophic large-volume landslide debris accompanying early caldera subsidence must be concealed at depth near the ring faults. The modeled height of a lithic-debris fan within the fill, needed to account for the collar volume, is approximately 2 km, suggesting total subsidence of 4–5 km. As at Crater Lake, the lithic debris inferred within the Creede caldera approaches 50% of the total caldera fill, even though only a few percent of the exposed fill is landslide breccia. Such a slide-breccia geometry is well exposed at other calderas noted previously, such as Lake City, Grizzly Peak, and Tucson Mountains.

Aira

Aira caldera, which subsided most recently at approximately 22000 radiocarbon years B.P. in response to eruption of 300 km^3 of magma as outflow Ito Tuff (Aramaki 1984; Nagaoka 1988), has been interpreted as a 20-km-diameter funnel caldera, based largely on gravity data (Yokoyama and Ohkawa 1986). It is a young, well-preserved representative of the many large calderas interpreted as funnel shaped in Japan. Geometric models for Aira caldera are impeded by lack of direct information on the nature of the caldera fill, collar geometry, diameter of the vent or subsided caldera core, and subsidence depth (all concealed beneath shallow water in Kagoshima Bay), as well as by probable structural complexities resulting from multiple confocal explosive eruptions (Nagaoka 1988). One model calculation for the Ito eruption and associated caldera subsidence (Fig. 4A; Table 1) is based on interpretation as a large funnel: a 20-km topographic diameter, a collar height of 2 km, and an average vent pipe (structural caldera) diameter of 6 km (from Fig. 18 in Aramaki 1984). This model would require a large proportion of fill by lithic debris (89%) and intracaldera accumulation of only approximately 8% of the total eruptive volume of tuff. Such a model seems unlikely; the indicated ratio of lithic fill to intracaldera tuff is much greater than that observed in eroded calderas of comparable size in Japan and elsewhere, the volume ratio of intracaldera to outflow tuff is lower, and the large funnel-vent diameter (10 km diameter in its upper part, as depicted by Aramaki) merges conceptually with a ring-fault boundary. Whatever the detailed subsidence structure, a large volume of caldera-wall material must remain within the caldera. Even though a prominent lithic-rich basal unit (Kamewarizaka breccia) underlies proximal outflow Ito tuff, its volume of as much as 15 km^3 (estimated from data in Aramaki 1984) is only 6% of the missing collar volume. If the lithic material

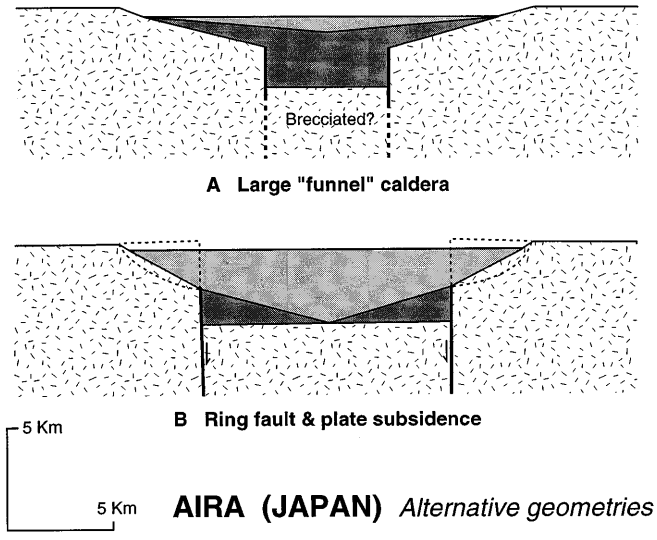

Fig. 4 Alternative scaled dimensions for Aira caldera, Japan, illustrating effects of ambiguities concerning its structural boundaries. At constant total subsidence depth, the proportions of intracaldera tuff and lithic breccia vary greatly in relation to inferred diameter of the subsided core. Assumptions and simplifications are the same as for Fig. 3. **A** Approximation of the funnel subsidence inferred by Aramaki (1984, Fig. 18), modified by using geometric simplifications from Fig. 1. **B** Alternative ring-fault geometry, comparable to exposures at Tertiary calderas of comparable size

derived from the collar were deposited mainly as a cone fan along an inner funnel wall (as modeled for ring-fault calderas; Fig. 1), the lithic debris would extend to the improbable depth of 12 km (see Appendix, model A-2).

These geometric problems at Aira and other Japanese calderas, such as Aso, Hakone, Kuttyaro, and Shikotsu, has led to the proposal that funnel calderas are excavated explosively, rather than by subsidence (Yokoyama 1983, 1987, 1991). Such an interpretation of caldera-forming processes is contradicted by the inadequate volumes of lithic fragments in the outflow tuffs from Aira and other well-preserved large calderas, as generally recognized since pioneering nineteenth century observations at Santorini by Fourqué and at Krakatau by Verbeek (Williams 1941; Self and Rampino 1982; McBirney 1990). Alternatively, the gravity interpretation for Aira may simply underestimate the diameter of the subsided caldera area, because caldera-wall slide debris, which would be more dense than infilling tuff, could be the dominant depositional units along margins of the structurally bounded depression. In contrast, a ring-fault interpretive model for Aira (Fig. 4B; Table 1), involving plate subsidence of a structural core 12 km in diameter (see Appendix, model A-3), yields values for proportions of intracaldera lithic and tuff fill comparable to eroded calderas of similar size.

La Garita

The enormous La Garita is considered representative of the largest ash-flow eruptions and caldera subsidence in the world. Other examples that are preserved in more pristine form but less well exposed in three dimensions include the 40- × 65-km 0.6-Ma Yellowstone caldera (Christiansen 1984) and the 35- × 60-km 4.1-Ma La Pacana caldera in northern Chile (Gardeweg and Ramirez 1987). The La Garita caldera formed at 27.8 Ma in response to eruption of the dacitic Fish Canyon tuff (5000 km^3 of magma) in the central San Juan volcanic field (Steven and Lipman 1976; Lipman et al. 1996). It is an elliptical caldera, approximately 35 × 75 km across at present erosion levels, that appears to be segmented into three subareas with differing collapse and postsubsidence features. Although the segmented caldera shape might suggest a multi-stage origin for the La Garita caldera, the outflow Fish Canyon tuff is a single ash-flow sheet characterized by a simple to weakly compound welding zonation, indicating depositions from a single sustained eruption. Resurgently uplifted intracaldera tuff is more than 1100 m thick in the La Garita Mountains (northern segment), with no base exposed; more than 700 m of intracaldera tuff is exposed, again without reaching the structural caldera floor, in canyons of the Piedra River in the nonresurgent southern segment. Although sparse lithic fragments are ubiquitous in the exposed intracaldera tuff, lenses of landslide breccia are rare in comparison with other deeply dissected San Juan calderas. After collapse, the La Garita caldera was filled to overflow by approximately 1.5 km of younger ash-flow sheets and lavas, indicating a minimum subsidence of more than 2.5 km. The scalloped map plan and relatively gentle slopes of the caldera walls indicate slumping enlargement of the topographic caldera comparable to that at smaller calderas such as Creede. For volumetric comparison with the smaller caldera examples, the strongly elliptical La Garita structure is modeled as having an average topographic diameter of 50 km (Fig. 3D), a structural diameter of 40 km, and subsidence depths of 3–5 km (see Appendix). Because of the great size of the La Garita caldera and large volume of intracaldera Fish Canyon tuff, the modeled proportion of lithic landslide debris derived from the collar area is notably lower than for the other caldera examples, probably only approximately 20% (Table 1; see Appendix). Little of this slide debris would have reached the central parts of the intracaldera fill that is exposed by resurgent uplift.

Overview

The geometric diversity of ash-flow calderas represents a continuum of features and processes bounded by a few simplified end members. Small calderas (< 3–5 km diameter) commonly have a *funnel geometry* because of dominant enlargement by slumping into an areally restricted vent; they merge with diatremes in geometry and eruptive style. Many larger calderas dominantly involve *plate (piston) collapse* of a coherent floor, bounded by steeply dipping ring faults; they are inferred to reflect voluminous eruptions from large shallow magma chambers. *Trap-door subsidence,* bounded by an incomplete ring fault and by a hinged segment, reflects early downsagging and incipient plate collapse related to smaller eruptions, an asymmetrical magma chamber, or regional tectonic influences. Deep magma chambers or small eruptive volumes may favor *downsag subsidence* without large bounding faults, although appearance of downsag can be generated by younger volcanic units draped over a pre-existing caldera or structural basin. Simple downsag calderas seem rare, but many plate-subsidence calderas contain inward-tilted blocks along their margins, as slices between bounding ring faults, or as incipient slide blocks incompletely detached from the inner topographic wall. Pervasively brecciated *chaotic disruption* of subsiding caldera floors is uncommon, at least at calderas more than a few kilometers across. Complex structures, with step-and-ramp block faulting, are common near caldera margins, even where central areas subside as a coherent plate. Pervasively disrupted caldera floors, broken by arcuate or rectilinear faults, commonly result from multiple nested or overlapping collapses during successive eruptions. Most calderas have such transitional attributes that subclassification can be inherently ambiguous and subjective. For example, the exceptionally

Appendix 1. Alternative models of key caldera elements and calculated volumes of intracaldera fill, based on a simplified geometric model (Figure 1). Italicized models are the preferred solutions that are utilized in Table 1

	Topo C diameter (km)	Structural diameter (km)	Subsidence depth (km)	Total collar height (km)	Collar slope, angle	Topo C area (km^2)	Structure area (km^2)	Structure volume (km^3)	Collar area (km^2)	Collar (lithic) volume (km^3)	Topo C volume (full) (km^3)	Collar percent (full)	Unfilled collar height (km)	Unfilled collar diameter (km)	Unfilled caldera volume (km^3)	Remaining caldera fill (km^3)	Tuff fill vol (km^3)	Caldera lithic fill (vol. %)	Lithic-fill height, margin (km)
Symbol	D	d	S	H	A	TCa	Sa	Sv	Ca	Cv	TCv	C%	h	Cud	Cuv	Cf	Tf	Cl	Lh
Formula	#	#	#	#	o	$\pi(D/d)^2$	$\pi(d/2)^2$	Sa*S	TCa-Sa	o	Sv + Cv	Cv/TCv ×100	#	o	o	TCv-Cuv	Cf-Cv	Cv/Cf ×100	3/2(Cv/Sa)
Caldera (estimated eruptive volume of magma)																			
Nigorikawa (3 km^3)																			
N-1	2.5	0.5	4.0	1.5	56	4.9	0.2	0.8	4.7	2.7	3.5	78	0.2	2.2	0.9	2.7	−0.1	104	21[a]
N-2	*2.5*	*0.5*	*6.0*	*1.5*	*56*	*4.9*	*0.2*	*1.2*	*4.7*	*2.7*	*3.9*	*70*	*0.2*	*2.2*	*0.9*	*3.0*	*0.3*	90	*21[a]*
N-3	2.5	0.5	8.0	1.5	56	4.9	0.2	1.6	4.7	2.7	4.3	64	0.2	2.2	0.9	3.4	0.7	80	21[a]
Crater Lake (80 km^3)																			
C-1	9.0	5.0	2.5	1.0	27	64	20	49	44	20	69	29	1.0	5.0	40	29	9.5	68	1.5
C-2	*9.0*	*5.0*	*3.0*	*1.0*	*27*	*64*	*20*	*59*	*44*	*20*	*79*	*25*	*1.0*	*5.0*	*40*	*39*	*19*	*51*	*1.5*
C-3	9.0	5.0	3.5	1.0	27	64	20	69	44	20	89	22	1.0	5.0	40	49	29.2	41	1.5
Aira (360 km^3: outflow only)																			
A-1	20	4.0	4.0	2.0	14	314	13	50	301	235	285	82	0.3	18	83	201	−33	116	28[a]
A-2	*20*	*6.0*	*4.0*	*2.0*	*16*	*314*	*28*	*113*	*286*	*235*	*348*	*67*	*0.3*	*18*	*85*	*263*	*28*	*89*	*12[a]*
A-3	*20*	*12.0*	*4.0*	*2.0*	*27*	*314*	*113*	*452*	*201*	*184*	*636*	*29*	*0.3*	*19*	*89*	*548*	*363*	*34*	*2*
Creede (500 km^3)																			
CR-1	24	14	4.0	2.0	22	452	154	615	298	272	888	31	1.5	17	489	399	127	68	2.7
CR-2	*24*	*14*	*4.5*	*2.0*	*22*	*452*	*154*	*692*	*298*	*272*	*965*	*28*	*1.5*	*17*	*489*	*476*	*204*	*57*	*2.7*
CR-3	24	14	5.0	2.0	22	452	154	7.09	298	272	1042	26	1.5	17	489	553	281	49	2.7
La Garita (5000 km^3)																			
LG-1	50	40	3.0	2.0	22	1963	1256	3768	707	681	4449	15	1.5	43	2526	1923	1242	35	0.8
LG-2	*50*	*40*	*4.0*	*2.0*	*22*	*1963*	*1256*	*5024*	*707*	*681*	*5705*	*12*	*1.5*	*43*	*2526*	*3179*	*2498*	*21*	*0.8*
LG-3	50	40	5.0	2.0	22	1963	1256	6280	707	681	6961	10	1.5	43	2526	4435	3754	15	0.8

NOTE: *Italicized are best-fit model parameters (used in Table 1)*

# indicates observed or estimated dimension (see Fig. 1)

Average collar slope angle (A) is calculated (rather than measured), because only small vertical portions of the concave-upward collar slopes are typically exposed in caldera walls. The calculated values is a minimum (see text)

Calculated lithic-fill height (Lh) assumes that the slide debris from the collar accumulates entirely within the structural caldera block (likely invalid for small funnel calderas); fill height is at structural margin

o indicates additional formulas: $A = \tan H/(D-d)$; $Cv = \pi H(D^3-3D*d^2+2d^3)/12(D-d)$; $Cud = d+(D-d)*(H-h)/H$; $Cuv = \pi h/12[(D^3-Cud^3)/(D-Cud)]$

[a] Improbable value; model least appropriate for small-diameter funnel geometry (see text for discussion)

well-exposed Grizzly Peak caldera in regional Colorado, originally described as a nested ring-fault plate-subsidence structure (Fridrich et al. 1991), has impressed others as involving significant downsag and piecemeal subsidence (Branney 1995). Interpreting caldera structures in terms of a continuum of subsidence styles, rather than as end-member types, can clarify relations between eruptive and structural processes in comparison with size of the eruption and geometry of the cogenetic magma chamber.

The flaring of inner caldera walls as a result of landsliding during subsidence is a major process in generating caldera morphology and caldera fill. Lithic material, derived from vent enlargement and slumping of caldera walls, is more voluminous in caldera fills than commonly recognized from study of young little-eroded calderas. In funnel calderas and small ring-fault subsidences, such lithic material is the dominant component of the caldera fill; model calculations suggest that some funnel calderas generate as great a volume of lithic debris as can be contained within the caldera (to the level of the unfilled collar height). In larger calderas, such as Crater Lake and Creede, wall-rock lithic fragments are roughly equal in volume to primary syncollapse volcanic ejecta that accumulate within the caldera. For the largest calderas, such as La Garita, the proportion of intracaldera slide debris is lower, and only minor slide material would be expected to reach central parts of the caldera fill that is exposed by resurgent doming. Thus, the size of magma chambers and volume of ash-flow eruptions strongly influence both caldera-subsidence processes and the lithologies of exposed intracaldera volcanic fill.

Acknowledgements Interpretations summarized herein were previously presented in part at the IAVCEI symposium "Large Volcanic Eruptions," convened by K. Hon and J. Pallister, at the 1995 IUGG meeting in Boulder, Colorado. C. Bacon provided helpful input on the geometry of Crater Lake caldera. T. Yamamoto and D. Miura helped obtain important recent Japanese publications. This work was supported by the Volcano Hazards Program of the U.S. Geological Survey. Revision of manuscript drafts benefited greatly from the thoughtful comments (and some divergent opinions) provided by C. Bacon, R. Bailey, M. Branney, R. Christiansen, W. Hildreth, J. Marti, and G. P. L. Walker.

References

Almond DC (1977) The Sabaloka igneous complex, Sudan. Phil Trans R Soc Lond 287:595–633

Ando S (1981) An example of the structure of Crater Lake-type caldera, Nigorikawa caldera, southwest Hokkaido, Japan. Abstracts, 1981 IAVCEI Symposium–Arc Volcanism, pp 9–10

Ankeny LA, Braile LW, Olsen KH (1986) Upper crustal structure beneath the Jemez Mountains volcanic field, New Mexico, determined by three-dimensional simultaneous inversion of seismic relraction and earthquake data. J Geophys Res 91:6188–6198

Aramaki S (1984) Formation of the Aira caldera, southern Kyushu, ~22000 years ago. J Geophys Res 89:8485–8501

Bacon CR (1983) Eruptive history of Mount Mazama and Crater Lake caldera, Cascade Range, USA. J Volcanol Geotherm Res 18:57–115

Bailey RA, Dalrymple GB, Lanphere MA (1976) Volcanism, structure, and geochronology of Long Valley caldera, Mono County, California. J Geophys Res 81:725–744

Baker MCW (1981) The nature and distribution of upper Cenozoic ignimbrite centres in the Central Andes. J Volcanol Geotherm Res 11:293–315

Bethke PM, Campbell WR, Hulen JB, Moses TH Jr (1994) Creede caldera continental scientific drilling program. Overview (abstr). Geol Soc Am (abstracts with programs) 26:398

Branney MJ (1995) Downsag and extension at calderas. New perspectives on collapse geometries from ice-melt-, mining, and volcanic subsidence. Bull Volcanol 57:303–318

Branney MJ, Gilbert JS (1995) Ice-melt collapse pits and associated features in the 1991 lahar deposits of Volcán Hudson, Chile. criteria to distinguish eruption-induced glacier melt. Bull Volcanol 57:293–302

Branney MJ, Kokelaar P (1994) Volcanotectonic faulting, soft-state deformation, and rheomorphism of tuffs during development of a piecemeal caldera, English Lake District. Geol Soc Am Bull 106:507–530

Buddington AF (1959) Granite emplacement with special reference to North America. Geol Soc Am Bull 70:671–747

Busby Sperra CJ (1984) Large-volume rhyolitic ash flow eruptions and submarine caldera collapse in the Lower Mesozoic Sierra Nevada, California. J Geophys Res 89:8417–8428

Carr WJ, Quinlivan WD (1968) Structure of Timber Mountain resurgent dome. Geol Soc Am Mem 110:99–108

Chesner CA, Rose WI (1991) Stratigraphy of the Toba tuffs and the evolution of the Toba caldera complex, Sumatra, Indonesia. Bull Volcanol 53:343–356

Christiansen RL (1984) Yellowstone magmatic evolution: its bearing on understanding large-volume explosive volcanism. In: Explosive volcanism: inception, evolution, and hazards. National Academy Press, Washington DC, pp 84–95

Christiansen RL, Lipman PW, Carr WJ, Byers FM Jr, Orkild PP, Sargent KA (1977) The Timber Mountain--Oasis Valley caldera complex of southern Nevada. Geol Soc Am Bull 88:943–959

Clough CT, Maufe HB, Bailey EB (1909) The cauldron-subsidence of Glen Coe, and the associated igneous phenomena. Q J Geol Soc Lond 65:611–678

Cunningham CG, Steven TA (1979) Mount Belknap and Red Hills calderas and associated rocks, Marysvale volcanic field, west-central Utah. US Geol Surv Bull 1468:1–33

Decker RW (1987) Dynamics of Hawaiian volcanoes: an overview. US Geol Surv Prof Pap 1350:997–1018

Dohnan Geothermal Energy Co. (1984) Geothermal development in the Nigorikawa area, Hokkaido, Japan. Company Report, 17 pp

Druitt T, Francaviglia V (1992) Caldera formation on Santorini and the physiography of the islands in the late Bronze Age. Bull Volcanol 54:484–493

Du Bray EA, Pallister JS (1991) An ash flow caldera in cross section. Ongoing field and geochemical studies of the mid-Tertiary Turkey Creek caldera, Chiricahua Mountains, SE Arizona. J Geophys Res 96 (13): 435–458

Du Bray EA, Pallister JS (1994) Geologic map of the Chiricahua Peak quadrangle Cochise County, Arizona. US Geol Surv Geol Quad Map GQ-1733

Dungan MA, Lipman PW, Colucci MT, Ferguson KM, Balsley SD (1989) Southeastern (Platoro) caldera complex. In: IAVCEI fieldtrip guide: Oligocene-Miocene San Juan volcanic field, Colorado. New Mexico Bur Mines Min Res Mem 46:305–329

Eaton GP et al. (1975) Magma beneath Yellowstone National Park. Science 188:787–796

Eichelberger JC, Hildreth W (1986) Research drilling at Katmai, Alaska. EOS, Trans Am Geophys Union 67:778–780

Emeleus CH, Gyopari MC (1992) Britsh Tertiary volcanic province. Chapman and Hall, London
Ferguson JF, Cogbill AH, Warren RG (1994) A geophysical–geological transect of the Silent Canyon caldera complex, Pahute Mesa, Nevada. J Geophys Res 99:4323–4340
Fiske RL, Tobisch OT (1994) Middle Cretaceous ash-flow tuff and caldera-collapse deposit in the Minarets caldera, east-central Sierra Nevada, California. Geol Soc Am Bull 106:582–593
Francis PW, McDonough WF, Hamil M, O'Callaghan LJ, Thorpe RS (1984) The Cerro Purico shield complex, North Chile. In: Harmon RS, Barreiro BA (eds) Andean magmatism–chemical and isotopic constraints, Shiva Publications, Nantwich, UK, pp 106–123
Fridrich CJ, Smith RP, DeWitt E, McKee EH (1991) Structural, eruptive, and intrusive evolution of the Grizzly Peak caldera, Sawatch Range, Colorado. Geol Soc Am Bull 103:1160–1177
Gardeweg PM, Ramirez CF (1987) The La Pacana caldera and the Atana ignimbrite: a major ash-flow and resurgent caldera complex in the Andes of northern Chile. Bull Volcanol 49:547–566
Gazis CA, Lanphere MA, Taylor HP Jr, Gurbanov A (1995) $^{40}Ar/^{39}Ar$ and $^{18}O/^{16}O$ studies of the Chegem ash-flow caldera and Eldjurta Granite: cooling of two late Pliocene igneous bodies in the Greater Caucasus Mountains, Russia. Earth Planet Sci Lett 134:377–391
Gudmundsson A (1988) Formation of collapse calderas. Geology 16:808–810
Halliman S (1993) Nonchaotic collapse at funnel calderas. Gravity study of the ring fractures at Guayabo caldera, Costa Rica. Geology 21:367–370
Hearn BC Jr (1966) Diatremes with kimberlitic affinities in north-central Montana. Science 159:622–625
Henry CD, Price JG (1984) Variations in caldera development in the Tertiary volcanic field of trans-Pecos Texas. J Geophys Res 89:8765–8786
Henry CD, Price JG (1989) The Christmas Mountains caldera complex, Trans-Pecos Texas: the geology and development of a laccocaldera. Bull Volcanol 52:97–112
Hildreth W (1987) New perspectives on the eruption of 1912 in the Valley of Ten Thousand Smokes, Katmai National Park, Alaska. Bull Volcanol 46:680–693
Hildreth W (1996) Kulshan caldera. A Quaternary subglacial caldera in the North Cascades, Washington. Geol Soc Am Bull: 108:786–793
Hildreth W, Mahood GA (1986) Ring-fracture eruption of the Bishop Tuff. Geol Soc Am Bull 97:396–403
Holcomb RT (1987) Eruptive history and long-term behavior of Kilauea Volcano. USÈGeol Surv Prof Pap 1350:261–350
Hon KA (1987) Geologic and petrologic evolution of the Lake City caldera, San Juan Mountains, Colorado. PhD thesis, Univ Colorado, 244 pp
Hon K, Fridrich C (1989) How calderas resurge (abstr). IAVCEI Abstracts, New Mexico Bur Mines Min Res Bull 131:135
Howells MF, Reedman AJ, Campbell DG (1986) The submarine eruption and emplacement of the Lower Rhyolitic tuff Formation (Ordovician), N Wales. J Geol Soc Lond 143:411–423
Imaoka T, Murakami N, Matsumoto T, Yamasaki H (1988) Paleogene cauldrons in the western San-in District, southwest Japan. J Fac Liberal Arts, Yamaguchi Univ 22:41–75 (in Japanese, with English abstract)
Iyer HM (1984) Geophysical evidence for the locations, shapes and sizes, and internal structures of magma chambers beneath regions of Quaternary Volcanism. Phil Trans R Soc Lond A310:473–510
Ito T, Utada M, Okuyama T (1989) Mio-Pliocene calderas in the Backbone region in northeast Japan. Mem Geol Soc Jap 32:409–429 (in Japanese, with English abstract)
John DA (1995) Tilted middle Tertiary ash-flow calderas and subjacent granitic plutons, southern Stillwater Range, Nevada. Cross sections of an Oligocene igneous center. Geol Soc Am Bull 107:180–200
Johnson CM, Shannon JR, Fridrich CJ (1989) Roots of ignimbrite calderas: batholithic plutonism, volcanism, and mineralization in the southern Rocky Mountains, Colorado and New Mexico. New Mex Bur Mines Mineral Resources Mem 46:275–302
Kamata H (1989) Shishimuta caldera, the buried source of the Yabakei pyroclastic flow in the Hohi Volcanic zone, Japan. Bull Volcanol 51:41–50
Kingsley L (1931) Cauldron subsidence of the Ossipee Mountains. Am J Sci 22:139–168
Komazawa M (1995) Gravimetric analysis of Aso Volcano and its interpretation. J Geodetic Soc Jap 41:17–45
Komuro H (1987) Experiments on cauldron formation. a polygonal cauldron and ring fractures. J Volcanol Geotherm Res 31:131–149
Komura H, Shichi R, Wada H, Itoi Y (1996) Basement relief under Sanbe caldera inferred from gravity anomaly. Bull Volcanol Soc Jap 41:1–10 (in Japanese, with English abstract)
Lambert MB (1974) The Bennett Lake cauldron subsidence complex, British Columbia and Yukon Territory. Geol Surv Can Bull 227:1–213
Lehman JA, Smith RB, Schilly MM (1982) Upper crustal structure of the Yellowstone caldera from seismic delay time analysis and gravity correlations. J Geophys Res 87:2713–2730
Lipman PW (1976) Caldera collapse breccias in the western San Juan Mountains, Colorado. Geol Soc Am Bull 87:1397–1410
Lipman PW (1984) The roots of ash-flow calderas in North America: windows into the tops of granitic batholiths. J Geophys Res 89:8801–8841
Lipman PW (1988) Evolution of silicic magma in the upper crust. the mid-Tertiary Latir Volcanic field and its cogenetic granitic batholith, northern New Mexico, USA. Trans R Soc Edinburgh 79:265–288
Lipman PW (1993) Geologic map of the Tucson Mountains caldera, Arizona. US Geol Surv Misc Invest Map I-2205, scale 1:48000
Lipman PW, Sawyer DA, Hon K (1989) Central San Juan caldera cluster. In: IAVCEI fieldtrip guide: Oligocene-Miocene San Juan volcanic field, Colorado. New Mexico Bur Mines Mineral Res Mem 46:330–350
Lipman PW et al. (1993) 2.8-Ma ash-flow caldera at Chegem River in the northern Caucasus Mountains (Russia), contemporaneous granites, and associated ore deposits. J Volcanol Geotherm Res 57:85–124
Lipman PW, Dungan MA, Brown LD, Deino A (1996) Recurrent eruption and subsidence at the Platoro caldera complex, southeastern San Juan volcanic field, Colorado. New tales from old tuffs. Geol Soc Am Bull 108:1039–1055
Luedke RG, Koeppen RP, Flores MA, Espinosa AO (1990) Reconnaissance geologic map of the Morococala volcanic field, Bolivia. US Geol Surv Misc Invest Map I-2014
Macdonald GA (1972) Volcanoes. Prentice Hall, New Jersey
Mahood GA (1980) Geological evolution of a Pleistocene rhyolitic center–Sierra La Primavera, Jalisco, Mexico. J Volcanol Geotherm Res 8: 199–230
Mahood GA, Hildreth W (1986) Geology of the peralkaline volcano at Pantelleria, Strait of Sicily. Bull Volcanol 48:143–172
Marti J, Ablay GJ, Redshaw LT, Sparks RSJ (1994) Experimental studies of collapse calderas. J Geol Soc Lond 151:919–929
Matumoto T (1943) The four gigantic caldera volcanoes of Kyushu. Jap J Geol Geogr 19:1–57
McBirney AR (1990) An historical note on the origin of calderas. J Volcanol Geotherm Res 42:303–306
Miura D (1997) Coherent caldera floor in a deeply dissected caldera: evaluation of its structure in relation to caldera formation, Miocene Kumano caldera, southwest Japan. Int Assoc Volcanol Chem Earth Interior, Abs Vol (Puerto Vallarta), p. 152
Mizugaki K (1993) Geologic structure and volcanic history of Sunagohara caldera volcano, Fukushima, Japan. J Geol Soc Jap 99:721–737 (in Japanese, with English abstract)

Mori J, McKee C, Itikarai I, Lowenstern P, Saint Ours P de, Talai B (1989) Earthquakes of the Rabaul seismo-deformational crisis, September 1983 to July 1985:seismicity on a caldera ring fault. In: Latter JH (edÖcchs256) Volcanic hazards. IAVCEI Proc Volcanol, vol 1, pp 429–462

Murakami H, Komuro H (1993) Sakugi cauldron–Paleogene cauldron in central Chugoku, southwest Japan. J Geol Soc Jap 99:243–254 (in Japanese, with English abstract)

Nagaoka S (1988) The late Quaternary tephra layers from the caldera volcanoes in and around Kagoshima Bay, southern Kyushu, Japan. Geogr Rep Tokyo Metropolitan Univ 23:49–122

Nairn IA, Wood CP, Bailey RA (1994) The Reporoa caldera, Taupo volcanic zone: source of the Kaingaroa ignimbrites. Bull Volcanol 56:529–537

Nairn IA, McKee CO, Talai B, Wood CP (1995) Geology and eruptive history of the Rabaul caldera area, Papua New Guinea. J Volcanol Geotherm Res 69:255–284

Nappi G, Renzulli A, Santi P (1991) Evidence of incremental growth in the Vulsinian calderas (central Italy). J Volcanol Geotherm Res 47:13–31

Nelson CH et al. (1994) The Volcanic, sedimentologic, and paleolimnologic history of the Crater Lake caldera floor, Oregon. Evidence for small caldera evolution. Geol Soc Am Bull 106:684–704

Oftedahl C (1978) Cauldrons of the Permian Oslo rift. J Volcanol Geotherm Res 3:343–372

Ort MH (1993) Eruptive processes and caldera formation in nested downsag-collapse caldera: Cerro Panizos, central Andes Mountains. J Volcanol Geotherm Res 56:221–252

Otake M, Sato H, Yamaguch Y (1997) Geologic development of the Late Miocene Tokusa caldera in the southern Aizu district, northeast Honshu, Japan. J Geol Soc Jap 103:1–20 (in Japanese, with English abstract)

Pierce Kl, Morgan LA (1992) The track of the Yellowstone hot spot: volcanism, faulting, and uplift. In: Link PK, Kuntz MA, Platt LB (eds) Regional geology of eastern Idaho and western Wyoming. Geol Soc Am Mem 179:1–53

Ponko SC, Sanders CO (1994) Inversion for P and S wave attenuation structure, Long Valley caldera, California. J Geophys Res 99:2619–2635

Reynolds DL (1956) Calderas and ring complexes. Verh K Ned Geol Mijnbouwkd Genoot 16:355–398

Roberts RM, Aki K, Fehler MC (1991) A low-velocity zone in the basement beneath Valles caldera, New Mexico. J Geophys Res 96:21583–21596

Rosi M, Vezzoli L, Aleotti P, Censi M de (1996) Interaction between caldera collapse and eruptive dynamics during the Campanian ignimbrite eruption, Phlegraean fields, Italy. Bull Volcanol 57:541–554

Rowley P, Anderson RE (1996) The syntectonic caldera: a new caldera type bounded by synchronous linear faults (abstrÖcchs256). Geol Soc Am (abstracts with programs) 28:449

Rytuba JJ, McKee EH (1984) Peralkaline ash flow tuffs and calderas of the McDermitt volcanic field, southeast Oregon and north central Nevada. J Geophys Res 89:8616–8628

Sanders CO (1984) Location and configuration of magma bodies beneath Long Valley, California, determined from anomalous earthquake signals. J Geophys Res 89:8287–8302

Sanders CO, Ponko SC, Nixon LD, Schwartz EA (1995) Seismological evidence for magmatic and hydrothermal structure in Long Valley caldera from local earthquake attenuation and velocity tomography. J Geophys Res 100:8311–8326

Sawada Y (1984) Subterranean structure of collapse caldera associated with andesitic and dacitic eruptions: structural evolution of the Miocene Kakeya cauldron, southwest Japan. Bull Volcanol 47:551–568

Sawyer DA, Fleck RJ, Lanphere MA, Warren RG, Broxton DE, Hudson MR (1994) Episodic caldera volcanism in the Miocene southwestern Nevada volcanic field: revised stratigraphic framework $^{40}Ar/^{39}Ar$ geochronology, and implications for magmatism and extension. Geol Soc Am Bull 106:1304–1318

Scandone R (1990) Chaotic collapse of calderas. J Volcanol Geotherm Res 42:285–302

Seager WR, McCurry M (1988) The cogenetic Organ cauldron and batholith, south central New Mexico: evolution of a large volume ash flow cauldron and its source magma chamber. J Geophys Res 93:4421–4433

Self S, Rampino MR (1982) Comments on "A geophysical interpretation of the 1883 Krakatau eruption" by I. Yokoyama. J Volcanol Geotherm Res 13:379–386

Self S, Goff FF, Gardner JN, Wright JV, Kite WM (1986) Explosive rhyolitic volcanism in the Jemez Mountains: vent location, caldera development and relation to regional structure. J Geophys Res 91:1779–1798

Sheridan MF (1978) The Superstition cauldron complex. Arizona Bur Geol Min Technol Spec Pap 2:85–96

Silva SL de (1989) Altiplano-Puna volcanic complex of the central Andes. Geology 17:1102–1106

Silva SL de (1997) Sources of ignimbrites in the Central Andes. Int Assoc Volcanol Chem Earth Interior, Abs Vol (Puerto Vallarta), p. 26

Silva SL de, Francis PW (1991) Volcanoes of the Central Andes. Springer, Berlin Heidelberg New York

Sparks RSJ, Francis PW, Hamer RD, Pankhurst RJ, O'Callaghan LO, Thorpe RS, Page R (1987) Ignimbrites of the Cerro Galan caldera, NW Argentina. J Volcanol Geotherm Res 24:205–248

Smith RL (1960) Ash flows. Geol Soc Am Bull 71:795–842

Smith RL, Bailey RA (1968) Resurgent cauldrons. Geol Soc Am Mem 116:83–104

Smith RB, Braille LW (1994) The Yellowstone hotspot. J Volcanol Geotherm Res 61:121–187

Steck LK, Prothero WA (1994) Crustal structure beneath Long Valley caldera from modeling of teleseismic P wave polarizations and Ps converted waves. J Geophys Res 99:6881–6898

Steck LK et al. (in press) Crust and upper mantle P-wave velocity structure beneath the Valles caldera, New Mexico: results from the JTEX teleseismic experiment. J Geophys Res

Steven TA, Lipman PW (1976) Calderas of the San Juan volcanic field, southwestern Colorado. US Geol Surv Prof Pap 958:1–35

Steven TA, Rowley PD, Cunningham CG (1984) Calderas of the Marysvale volcanic field, west central Utah. J Geophys Res 89:8751–8764

Takada A (1987) Development of the Shitara igneous complex, central Japan, and the structure of its cauldrons. J Geol Soc Jap 93:167–184 (in Japanese, with English abstract)

Takahashi M (1986) Anatomy of a Middle Miocene Valles-type caldera cluster. Geology of the Okueyama volcano-plutonic complex, southwest Japan. J Volcanol Geotherm Res 29:33–70

Tilling RI, Koyanagi RY, Lipman PW, Lockwood JP, Moore JG, Swanson DA (1976) Earthquake and related catastrophic events, Island of Hawaii, November 29, 1975:a preliminary report. US Geol Surv Circ 740:1–33

Varga RJ, Smith BM (1984) Evolution of the early Oligocene Bonanza caldera, northeast San Juan volcanic field, Colorado. J Geophys Res 89:8679–8694

Walker GPL (1984) Downsag calderas, ring faults, caldera sizes, and incremental caldera growth. J Geophys Res 89:8407–8416

Walker GPL (1985) Origin of coarse lithic breccias near ignimbrite source vents. J Volcanol Geotherm Res 25:157–172

Walker GPL (1988) Three Hawaiian calderas: an origin through loading by shallow intrusions? J Geophys Res 93:14773–14784

Williams H (1941) Calderas and their origin. Univ California Publ Depart Geol Sci 25:239–346

Williams H (1942) The geology of Crater Lake National Park, Oregon. Carnegie Inst Washington Publ 540:1–162

Williams H, McBirney AR (1979) Volcanology. Freeman, Cooper and Co, San Francisco

Wilson CJN, Rogan AM, Smith IEM, Northey DJ, Nairn IA, Houghton BF (1984) Caldera volcanoes of the Taupo volcanic zone, New Zealand. J Geophys Res 89:8436–8484

Wisser E (1927) Oxidation subsidence at Bisbee, Arizona. Econ Geol 22:761–790

Yamada E (1975) Geological development of the Onikobe caldera and its hydrothermal system. Proc UN Symp Develop Use Geotherm Resources, 2:665–672

Yamamoto T (1991) Large scale slope failure during caldera collapse: structural development of the Late Miocene Takagawa caldera, northeast Japan. Bull Volcanol Soc Japan 36:1–10 (in Japanese, with English abstract)

Yamamoto T (1992a) Chronology of the late Miocene-Pleistocene caldera volcanoes in the Aizu district, northeast Japan. J Geol Soc Jap 98:21–38 (in Japanese, with English abstract)

Yamamoto T (1992b) The middle Pleistocene explosive volcanism in Sunagohara caldera volcano, Aizu, Japan: evidence from non-marine volcaniclastic facies of the Todera formation. J Geol Soc Jap 99:721–737 (in Japanese, with English abstract)

Yamamoto T (1994) Structural development and eruptive history of late Miocene to Pliocene caldera volcanoes in the Inawashiro district, NE Japan. Bull Geol Surv Jap 45:135–155 (in Japanese, with English abstract)

Yokoyama S (1983) Gravimetric studies and drilling results at the four calderas in Japan. Arc volcanism: physics and tectonics, Terra Sci Publ Co, Tokyo, pp 29–41

Yokoyama S (1987) A quantitative consideration of several calderas for study of their formation. Geofisica Int 26:487–498

Yokoyama S, Ohakawa S (1986) Subsurface structure of Aira caldera and its vicinity in southern Kyushu, Japan. J Volcanol Geotherm Res 30:253–282

Yokoyama S, Mena M (1991) Structure of La Primavera caldera, Jalisco, Mexico. J Volcanol Geotherm Res 47:183–194

Yoshida T (1984) Tertiary Ishizuchi cauldron, southwest Japan arc. J Geophys Res 89:8502–8510